© 2015. Published by The Company of Biologists Ltd | Development (2015) 142, 3801 doi:10.1242/dev.131821

CORRECTION

Crucial requirement of ERK/MAPK signaling in respiratory tract development

Olivier Boucherat, Valérie Nadeau, Félix-Antoine Bérubé-Simard, Jean Charron and Lucie Jeannotte

There was an error published in *Development* **141**, 3197-3211.

In the key for Fig. 3C, the grey bars were labelled with the incorrect genotype name. The correct genotype is *Mek1*$^{+/flox}$;*Mek2*$^{-/-}$;*Dermo1*$^{+/cre}$. This error does not affect the conclusions of the paper.

The authors apologise to readers for this mistake.

© 2014. Published by The Company of Biologists Ltd | Development (2014) 141, 3197-3211 doi:10.1242/dev.110254

RESEARCH ARTICLE

Crucial requirement of ERK/MAPK signaling in respiratory tract development

Olivier Boucherat[1], Valérie Nadeau[1], Félix-Antoine Bérubé-Simard[1], Jean Charron[1,2,*] and Lucie Jeannotte[1,2,*]

ABSTRACT

The mammalian genome contains two ERK/MAP kinase genes, *Mek1* and *Mek2*, which encode dual-specificity kinases responsible for ERK/MAP kinase activation. In order to define the function of the ERK/MAPK pathway in the lung development in mice, we performed tissue-specific deletions of *Mek1* function on a *Mek2* null background. Inactivation of both *Mek* genes in mesenchyme resulted in several phenotypes, including giant omphalocele, kyphosis, pulmonary hypoplasia, defective tracheal cartilage and death at birth. The absence of tracheal cartilage rings establishes the crucial role of intracellular signaling molecules in tracheal chondrogenesis and provides a putative mouse model for tracheomalacia. *In vitro*, the loss of *Mek* function in lung mesenchyme did not interfere with lung growth and branching, suggesting that both the reduced intrathoracic space due to the dysmorphic rib cage and the omphalocele impaired lung development *in vivo*. Conversely, *Mek* mutation in the respiratory epithelium caused lung agenesis, a phenotype resulting from the direct impact of the ERK/MAPK pathway on cell proliferation and survival. No tracheal epithelial cell differentiation occurred and no SOX2-positive progenitor cells were detected in mutants, implying a role for the ERK/MAPK pathway in trachea progenitor cell maintenance and differentiation. Moreover, these anomalies were phenocopied when the *Erk1* and *Erk2* genes were mutated in airway epithelium. Thus, the ERK/MAPK pathway is required for the integration of mesenchymal and epithelial signals essential for the development of the entire respiratory tract.

KEY WORDS: *Mek* gene function, ERK/MAPK pathway, Lung morphogenesis, Lung agenesis, Trachea, Omphalocele

INTRODUCTION

Lung development is an orchestrated process directed in part by mesenchymal-epithelial interactions that rely on paracrine signaling mediated by secreted ligands and cell-cell contacts. How signal instructions are interpreted to ultimately control cell fate and morphogenesis remains an open question in lung biology. The mitogen-activated protein kinase (MAPK) pathways are involved in signal transduction through transmembrane receptors. They consist of protein kinase cascades linking extracellular stimuli to targets scattered throughout the cell to generate specific cellular responses to environmental changes. The classical extracellular signal-regulated kinase ERK/MAPK pathway constitutes the major cascade for the control of cell proliferation, differentiation and survival. It transduces the effects of growth factors implicated in cell fate determination and developmental processes. In mammals, the ERK/MAPK pathway contains the MEK1 and MEK2 kinases that activate ERK1 and ERK2. The high sequence homology between MEK1 and MEK2 and the sharing of common activation mechanisms suggest that they are functionally redundant (Raman et al., 2007). However, the loss of *Mek1* (*Map2k1* – Mouse Genome Informatics) function in mice results in embryonic death due to placenta defects, whereas *Mek2* (*Map2k2* – Mouse Genome Informatics) mutant mice do not show a phenotype (Bélanger et al., 2003; Giroux et al., 1999). *Mek1*$^{+/-}$; *Mek2*$^{+/-}$ embryos die from abnormal placenta development, revealing the importance of *Mek2* for proper placentation (Nadeau et al., 2009). The embryonic death of *Mek1*;*Mek2* mutants precludes the study of their function at later stages. Using a *Mek1* conditional allele and lineage-specific *Cre* mice, the function of both MEK1 and MEK2 proteins in numerous processes has been unveiled, highlighting the broad role of the ERK/MAPK pathway throughout life (Li et al., 2012; Newbern et al., 2008; Scholl et al., 2007; Yamashita et al., 2011).

In mice, lung formation starts with the outgrowth of the ventral foregut endoderm into the flanking mesenchyme to form the laryngotracheal groove. The tracheal rudiment then elongates caudally and bifurcates to form the two primary bronchi. During the pseudoglandular stage, numerous rounds of dichotomous branching produce the bronchial tree (Metzger et al., 2008). The subsequent canalicular and saccular phases lead to the thinning of lung mesenchyme, the differentiation of the distal epithelium and the formation of the vascular network, with the establishment of the air-blood barrier. After birth, alveoli formation increases the gas exchange surface to meet the requirements of the organism (Morrisey and Hogan, 2010). *In vivo* and *in vitro* experiments have revealed the importance of growth factors trafficking via MAPK pathways throughout lung development, including members of the fibroblast growth factor (FGF) family, such as FGF1, -2, -7, -9, -10 and -18, the platelet-derived growth factor A (PDGFA) and the epidermal growth factor (EGF). Despite the accumulating knowledge about the role of growth factors in lung morphogenesis, the downstream signaling events remain largely uncharacterized. The p38/MAPK pathway has been identified as a key player in the control of bud morphogenesis (Liu et al., 2008). Conversely, the implication of the ERK/MAPK pathway in lung morphogenesis has been suspected without ever being clearly demonstrated. *In vitro* treatment of fetal rat lung explants with a MEK inhibitor reduced branching and caused mesenchymal cell apoptosis that impaired explant growth (Kling et al., 2002). Moreover, the targeted expression in the developing lung epithelium of the activated forms of K-Ras or B-Raf, two kinases located upstream of MEK, affected normal airway shape in mice (Tang et al., 2011).

To define the role of the ERK/MAPK pathway in lung development, we specifically ablated *Mek1* function in the mesenchyme and epithelium on a *Mek2* null background. Deletion of all four *Mek* alleles in the mesenchyme caused multiple phenotypes, including

[1]Centre de recherche sur le cancer de l'Université Laval, Centre Hospitalier Universitaire de Québec, L'Hôtel-Dieu de Québec, Québec, Canada G1R 2J6. [2]Department of Molecular Biology, Medical Biochemistry and Pathology, Université Laval, Québec, Canada G1V 0A6.

*Authors for correspondence (jean.charron@crhdq.ulaval.ca; lucie.jeannotte@crhdq.ulaval.ca)

Received 17 March 2014; Accepted 16 June 2014

Development (2014) 141, 3197-3211 doi:10.1242/dev.110254

omphalocele, kyphosis, lung hypoplasia, abnormal trachea patterning and death at birth. The rescue of the branching defect in mutant lung explant cultures suggests that reduced intrathoracic space contributes to the lung phenotype. Wild-type lung explants exposed to MEK inhibitor exhibited less branching, thereby suggesting a role for MEK in lung epithelium. This was directly addressed by the *Mek* conditional deletion in the respiratory epithelium with the *Shh*^{cre} strain. *Mek1*$^{flox/flox}$;*Mek2*$^{-/-}$;*Shh*$^{+/Cre}$ embryos presented lung agenesis and no tracheal epithelial cell differentiation, phenotypes also seen in *Erk1*$^{-/-}$;*Erk2*$^{flox/flox}$;*Shh*$^{+/Cre}$ specimens. Thus, the ERK/MAPK pathway integrates distinct signals in the lung epithelium and the flanking mesenchyme that are essential for the correct respiratory tract formation.

RESULTS

Mek1 mesenchymal inactivation in a *Mek2* null background causes pulmonary hypoplasia

Ablation of *Mek1* function in the mesenchyme was produced with the *Dermo1*^{cre} deleter mouse line (supplementary material Fig. S1A-D). The *Mek1* mesenchymal deletion on a *Mek2* null background caused death at birth of all *Mek1*$^{flox/flox}$;*Mek2*$^{-/-}$;*Dermo1*$^{+/Cre}$ pups, which also showed reduced body size (Table 1). Comparison of the body weight of embryonic (E) day 18.5 embryos showed that the mesenchymal loss of all *Mek* alleles led to a ∼38% decrease in weight, thus indicating intrauterine growth restriction, a disorder due to placental underdevelopment (Fig. 1A; supplementary material Fig. S2A-F). *Mek1*$^{+/flox}$;*Mek2*$^{-/-}$;*Dermo1*$^{+/Cre}$ and *Mek1*$^{flox/flox}$;*Mek2*$^{+/-}$;*Dermo1*$^{+/Cre}$ mice did not show obvious phenotypes. Conversely, *Mek1*$^{flox/flox}$;*Mek2*$^{-/-}$;*Dermo1*$^{+/Cre}$ embryos displayed severe fully penetrant malformations, such as eyelid closure defect and giant omphalocele, a protrusion of the gut and liver outside the abdomen resulting from the incomplete closure of the ventral body wall (Fig. 1B-G; Christison-Lagay et al., 2011). *Mek1*$^{flox/flox}$;*Mek2*$^{-/-}$;*Dermo1*$^{+/Cre}$ mice died at birth, most likely from the cannibalization of the omphalocele by the mother. Alcian Blue staining of E15.5 mutants revealed the important disorganization of the axial skeleton, including kyphosis, which might contribute to the reduced space in the thoracic cavity (Fig. 1D; supplementary material Fig. S2G-R).

Mek1$^{flox/flox}$;*Mek2*$^{-/-}$;*Dermo1*$^{+/Cre}$ pups had smaller lungs with narrower airspaces and a thicker mesenchyme indicative of a delayed development (Fig. 2A-D). Lung hypoplasia was confirmed at E18.5, as the lung weight/body weight ratio corresponded to ∼67% of that of controls (Fig. 2E). To identify the factors contributing to hypoplasia, we measured lung cell proliferation and apoptosis. At E15.5, the number of phospho-histone H3 (pHH3)-positive mesenchymal cells was significantly reduced in *Mek1*$^{flox/flox}$;*Mek2*$^{-/-}$;*Dermo1*$^{+/Cre}$ mutants, whereas no difference was observed in epithelium (Fig. 2F-H). Similarly, the number of apoptotic cells was significantly augmented in the mesenchyme of *Mek1*$^{flox/flox}$;*Mek2*$^{-/-}$;*Dermo1*$^{+/Cre}$ specimens (Fig. 2I-K). The imbalance in the proliferation/apoptosis ratio in lung mesenchyme of *Mek1*$^{flox/flox}$;*Mek2*$^{-/-}$;*Dermo1*$^{+/Cre}$ embryos underlined the reduced mesenchymal area observed (Fig. 2L). As decreased lung branching may also contribute to hypoplasia, we evaluated the number of acini at E15.5, as, at this stage, the ramifying bronchial tree gives rise to epithelial tubular branches ending in terminal acini (Kotecha, 2000). Lungs from *Mek1*$^{flox/flox}$;*Mek2*$^{-/-}$;*Dermo1*$^{+/Cre}$ embryos displayed a decreased number of acini, indicating a defective branching process (Fig. 2M). Thus, insufficient proliferation, augmented apoptosis and decreased branching contributed to lung hypoplasia in *Mek1*$^{flox/flox}$;*Mek2*$^{-/-}$;*Dermo1*$^{+/Cre}$ embryos.

Normal cell differentiation and vascular development in lungs from *Mek1*$^{flox/flox}$;*Mek2*$^{-/-}$;*Dermo1*$^{+/Cre}$ embryos

To test whether lung cell differentiation requires ERK/MAPK mesenchymal activity, we monitored the expression of cell-specific markers at E18.5. Although *Mek1*$^{flox/flox}$;*Mek2*$^{-/-}$;*Dermo1*$^{+/Cre}$ embryos exhibited abnormally compact lungs with poorly developed saccules, no evident difference was observed for the secretory club (Clara) cells and the alveolar type I and type II pneumocytes with the markers CC10, T1α (podoplanin) and pro-SPC, respectively (supplementary material Fig. S3A-F). The distribution of capillary endothelial cells detected with PECAM also appeared normal. Smooth muscle cells positive for α-SMA were correctly localized around the bronchi and the large blood vessels (supplementary material Fig. S3G-J). We investigated by quantitative RT-PCR (qRT-PCR) the expression levels of stromal cell markers: desmin (*Des*) and transgelin (*Tagln*) for smooth muscle cells, *Pdgfrα* for myofibroblasts and *Pdgfrβ* for pericytes (Lindahl et al., 1997; Rock et al., 2011; Tada et al., 2007). Expression of *Hoxa5* and

Table 1. Ratios of genotypes in litters from crosses between *Mek1*$^{+/flox}$;*Mek2*$^{+/-}$;*Dermo1*$^{+/Cre}$ and *Mek1*$^{flox/flox}$;*Mek2*$^{-/-}$ mice

			***Mek1*$^{+/flox}$;*Mek2*$^{+/-}$;*Dermo1*$^{+/Cre}$ x *Mek1*$^{flox/flox}$;*Mek2*$^{-/-}$**							
			***Dermo1*$^{+/+}$**				***Dermo1*$^{+/Cre}$**			
Age	# of litters	# of pups	***Mek1*$^{+/flox}$ *Mek2*$^{+/-}$**	***Mek1*$^{+/flox}$ *Mek2*$^{-/-}$**	***Mek1*$^{flox/flox}$ *Mek2*$^{+/-}$**	***Mek1*$^{flox/flox}$ *Mek2*$^{-/-}$**	***Mek1*$^{+/flox}$ *Mek2*$^{+/-}$**	***Mek1*$^{+/flox}$ *Mek2*$^{-/-}$**	***Mek1*$^{flox/flox}$ *Mek2*$^{+/-}$**	***Mek1*$^{flox/flox}$ *Mek2*$^{-/-}$**
Expected (%)			(12.5)	(12.5)	(12.5)	(12.5)	(12.5)	(12.5)	(12.5)	(12.5)
E14.5	4	33	3 (10)	4 (12)	4 (12)	4 (12)	4 (12)	4 (12)	5 (15)	5 (15)
Omphalocele			0	0	0	0	0	0	0	4
E15.5	9	57	4 (7)	11 (19)	12 (21)	2 (4)	4 (7)	8 (14)	8 (14)	8 (14)
Omphalocele			0	0	0	0	0	0	0	8
E18.5	21	112	16 (14)	12 (12)	9 (8)	11 (10)	18 (16)	15 (13)	16 (14)	15 (13)
Omphalocele			0	0	0	0	0	0	0	15
Eyelid closure defect			0	0	0	0	0	0	0	15
D0	1	7	1 (14)	0 (0)	1 (14)	0 (0)	1 (14)	0 (0)	2 (29)	2* (29)
Omphalocele			0	0	0	0	0	0	0	2
Eye-open-at-birth			0	0	0	0	0	0	0	2
D21	6	39	3 (8)	7 (18)	6 (15)	9 (23)	2 (5)	3 (8)	9 (23)	0 (0)

* **Dead**

Development (2014) 141, 3197-3211 doi:10.1242/dev.110254

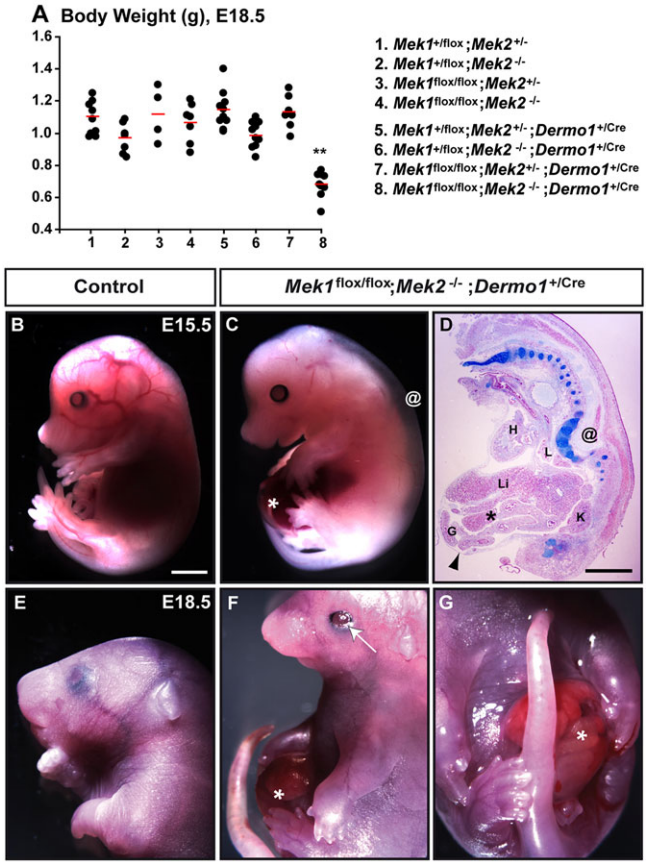

Fig. 1. *Mek* mesenchymal mutations affect intrauterine growth and cause multiple phenotypes. (A) Body weight of E18.5 control and *Mek1*$^{flox/flox}$;*Mek2*$^{-/-}$;*Dermo1*$^{+/Cre}$ embryos. The body weight value of *Mek1*$^{flox/flox}$;*Mek2*$^{-/-}$;*Dermo1*$^{+/Cre}$ was significantly reduced. (B-G) Gross morphology of E15.5 and E18.5 control and *Mek1*$^{flox/flox}$;*Mek2*$^{-/-}$;*Dermo1*$^{+/Cre}$ mouse embryos. Omphaloceles, indicated by asterisks, were present in *Mek1*$^{flox/flox}$;*Mek2*$^{-/-}$;*Dermo1*$^{+/Cre}$ embryos at both time points. (D) Alcian Blue- and nuclear Fast Red-stained sagittal sections of E15.5 *Mek1*$^{flox/flox}$;*Mek2*$^{-/-}$;*Dermo1*$^{+/Cre}$ embryo. The ventral extrusion of abdominal organs (liver and gut) covered by a thin membrane (arrowhead) is observed. @ in C,D indicate malformations of the vertebral column. Arrow in F indicates eyelid closure defect. G, gut; H, heart; K, kidney; L, lung; Li, liver. Scale bars: 2 mm (B-G).

Wnt2 genes, two mesenchyme-expressed regulators of lung development, was also analyzed (Boucherat et al., 2013; Morrisey and Hogan, 2010). No difference was observed except for *Des* and *Pdgfrα* expression (supplementary material Fig. S3K). Thus, cell differentiation appeared to occur normally along the respiratory tract in absence of a functional ERK/MAPK cascade in lung mesenchyme.

Molecular repercussions of the mesenchymal inactivation of *Mek* genes in the developing lung

We validated *Mek1* inactivation in lung mesenchyme from *Mek1*$^{flox/flox}$;*Mek2*$^{-/-}$;*Dermo1*$^{+/Cre}$ specimens by analyzing MEK protein expression (supplementary material Fig. S4A-D). In E15.5 controls, MEK1 and MEK2 proteins showed ubiquitous expression in the epithelial and mesenchymal compartments along the entire respiratory tract. In mutants, no MEK1 mesenchymal expression was detected, except for a few cells, and MEK1 epithelial expression remained unchanged. No MEK2 expression was seen in these mutants. To assess the impact of the *Mek* mutation on ERK activation, we monitored phospho-ERK (pERK) expression (supplementary material Fig. S4E,F). In controls, immunostaining was detected in mesenchymal cells flanking tubules undergoing branching and in a few epithelial cells. Conversely, in *Mek1*$^{flox/flox}$;*Mek2*$^{-/-}$;*Dermo1*$^{+/Cre}$ specimens, pERK was barely detectable in the mesenchyme, supporting the notion that MEK1 and MEK2 are the only kinases activating ERK1 and ERK2 in lung mesenchyme. Surprisingly, a strong pERK staining was detected in lung epithelium, suggesting deregulated cross-talk of the ERK/MAPK pathway between the tissue layers.

Microarray analysis of RNA extracted from lungs of E15.5 *Dermo1*$^{+/Cre}$, *Mek1*$^{+/flox}$;*Mek2*$^{-/-}$;*Dermo1*$^{+/Cre}$ and *Mek1*$^{flox/flox}$;*Mek2*$^{-/-}$;*Dermo1*$^{+/Cre}$ embryos was performed to evaluate the molecular impact of the mesenchymal loss-of-all *Mek* alleles on lung development. Venn diagrams displaying the total number of up- or downregulated transcripts with $P<0.05$ revealed that the number of differentially expressed transcripts between the *Mek1*$^{flox/flox}$;*Mek2*$^{-/-}$;*Dermo1*$^{+/Cre}$ experimental group and the *Dermo1*$^{+/Cre}$ control group was higher than that obtained when *Mek1*$^{+/flox}$;*Mek2*$^{-/-}$;*Dermo1*$^{+/Cre}$ and *Dermo1*$^{+/Cre}$ groups were compared (Fig. 3A). Thus, the mesenchymal loss of all *Mek* alleles had a greater influence on the lung transcriptome than the absence of three *Mek* alleles, which correlated with the phenotype observed.

A DAVID (Database for Annotation, Visualization and Integrated Discovery) functional annotation chart algorithm was used to identify the major biological processes modulated in mutant lungs (Huang et al., 2009). Upregulated genes in the *Mek1*$^{flox/flox}$;*Mek2*$^{-/-}$;*Dermo1*$^{+/Cre}$ group were associated with chromatin organization, metabolism, cell structure and motility, cell signaling, cell proliferation, differentiation and development, whereas downregulated genes were enriched for metabolism, cell proliferation, cell organization, biosynthetic processes and protein folding (supplementary material Fig. S5). In the *Mek1*$^{+/flox}$;*Mek2*$^{-/-}$;*Dermo1*$^{+/Cre}$ group, only genes associated with chromatin organization were upregulated, whereas genes related to metabolism and RNA processing were downregulated, indicating a broader impact of the four *Mek* alleles mutation on biological processes (data not shown).

A heat map was established with genes exhibiting a ≥1.5-fold change (Fig. 3B). As expected, *Mek2* transcripts were downregulated in *Mek1*$^{+/flox}$;*Mek2*$^{-/-}$;*Dermo1*$^{+/Cre}$ and *Mek1*$^{flox/flox}$;*Mek2*$^{-/-}$;*Dermo1*$^{+/Cre}$ groups. Downregulation of genes involved in cell proliferation, such as *Cdca3*, *Taf15*, *Egr1* and *Ccl21*, and upregulation of *Ddit4*, a gene associated with apoptosis, were detected in *Mek1*$^{flox/flox}$;*Mek2*$^{-/-}$;*Dermo1*$^{+/Cre}$ lungs, concurring with the lung phenotype observed (Ayad et al., 2003; Yoshida et al., 2010). Expression of genes implicated in lung development was also affected, such as *R-spondin 2 homolog* (*Rspo2* – Mouse Genome Informatics), a ligand acting through the Wnt canonical pathway, and TRIC-B (*Marveld2* – Mouse Genome Informatics), a monovalent cation-specific channel crucial for lung maturation (Bell et al., 2008; Yamazaki et al., 2009). The expression of selected candidates was confirmed by qRT-PCR and/or immunohistochemistry (IHC), validating the microarray results. For instance, expression of the *Scgb3a2* gene, encoding a growth factor and anti-apoptotic agent expressed in airways that promotes fetal lung development, was decreased in mutants (Fig. 3C-E; Kurotani et al., 2008). Expression of *Klf5*, encoding an epithelial transcription factor required for perinatal lung morphogenesis and known to activate ERK/MAPK signaling, was augmented in mutant lungs (Fig. 3C; Wan et al., 2008; Yang et al., 2007).

Expression of *Mkk6* (*Map2k6* – Mouse Genome Informatics), encoding the upstream activator of the p38/MAP kinase (*Mapk14* – Mouse Genome Informatics), was diminished in *Mek1*$^{flox/flox}$;*Mek2*$^{-/-}$;*Dermo1*$^{+/Cre}$ specimens (Fig. 3C). It impacted on p38/MAPK

Development (2014) 141, 3197-3211 doi:10.1242/dev.110254

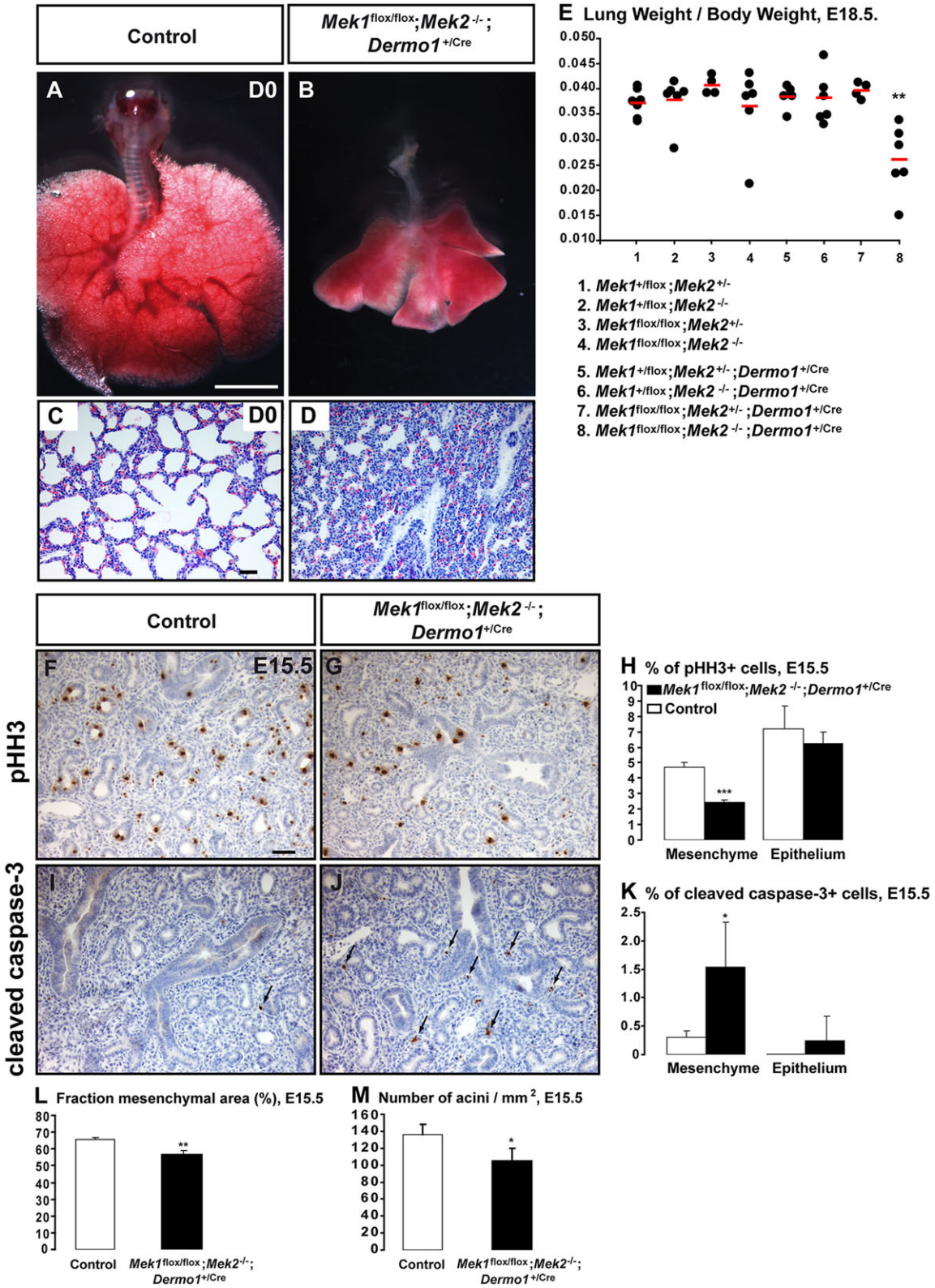

Fig. 2. Lung hypoplasia in *Mek1*$^{flox/flox}$;*Mek2*$^{-/-}$;*Dermo1*$^{+/Cre}$ neonates. (A,B) Macroscopic views showing the hypoplastic *Mek1*$^{flox/flox}$;*Mek2*$^{-/-}$;*Dermo1*$^{+/Cre}$ lung phenotype at D0 compared with lungs from littermate controls. (C,D) H&E-stained lung sections showed decreased sacculation and mesenchymal thickening in *Mek1*$^{flox/flox}$;*Mek2*$^{-/-}$;*Dermo1*$^{+/Cre}$ specimens. (E) The lung weight/body weight ratio was decreased by 33% in E18.5 *Mek1*$^{flox/flox}$;*Mek2*$^{-/-}$;*Dermo1*$^{+/Cre}$ embryos, thus confirming lung hypoplasia. (F-H) pHH3 IHC showed that proliferation was decreased in lung mesenchyme from E15.5 *Mek1*$^{flox/flox}$;*Mek2*$^{-/-}$;*Dermo1*$^{+/Cre}$ mutants. (I-K) Cleaved caspase 3 IHC showed increased apoptosis in lung mesenchyme from E15.5 *Mek1*$^{flox/flox}$;*Mek2*$^{-/-}$;*Dermo1*$^{+/Cre}$ mutants. Arrows indicate cleaved caspase 3-positive cells. (L,M) Quantitative morphometry of lungs from *Mek1*$^{flox/flox}$;*Mek2*$^{-/-}$;*Dermo1*$^{+/Cre}$ and controls at E15.5. Fraction of mesenchyme area (L) and number of acini per mm^2 (M) were significantly reduced in *Mek1*$^{flox/flox}$;*Mek2*$^{-/-}$;*Dermo1*$^{+/Cre}$ lungs. (*n*=4-5/group). Values are expressed as mean±s.d. Scale bars: 2 mm (A,B), 50 µm (C,D,F,G,I,J).

Development (2014) 141, 3197-3211 doi:10.1242/dev.110254

activation as shown by the reduced phospho-p38 (p-p38) expression in lung epithelium from mutants (Fig. 3F,G). As p38/MAP kinase is involved in lung branching, decreased p38 activation might contribute to the branching defect observed in *Mek1*$^{flox/flox}$;*Mek2*$^{-/-}$;*Dermo1*$^{+/Cre}$ mutants (Liu et al., 2008).

Many genes with altered expression in *Mek1*$^{flox/flox}$;*Mek2*$^{-/-}$;*Dermo1*$^{+/Cre}$ mutants are expressed in lung epithelium, implying that the loss of mesenchymal *Mek* function influenced epithelial behavior. However, the presence of thoracic cage deformities accompanied by omphalocele in *Mek1*$^{flox/flox}$;*Mek2*$^{-/-}$;*Dermo1*$^{+/Cre}$ embryos made it difficult to distinguish between the impact on gene expression due to the complete loss of *Mek* function and the genes dysregulated following physical interferences.

Pulmonary hypoplasia in *Mek1*$^{flox/flox}$;*Mek2*$^{-/-}$;*Dermo1*$^{+/Cre}$ specimens: a secondary consequence?

Impairment of fetal breathing movements, inadequate volume of amniotic fluid and reduced intrathoracic space can cause lung hypoplasia (Kotecha, 2000). To examine whether impaired lung development in *Mek1*$^{flox/flox}$;*Mek2*$^{-/-}$;*Dermo1*$^{+/Cre}$ was due to the physical repercussions of omphalocele and abnormal skeleton, we cultured whole-lung explants from E12.5 embryos, as, at this age, omphalocele was not apparent. At day (D) 0, lung primordia from controls and *Mek1*$^{flox/flox}$;*Mek2*$^{-/-}$;*Dermo1*$^{+/Cre}$ embryos had similar sizes. As expressed by the percentage in increase of distal branching between D0 and D1, D2 and D3, *Mek1*$^{flox/flox}$;*Mek2*$^{-/-}$;*Dermo1*$^{+/Cre}$ explants showed an increased branching and complexity comparable to controls (Fig. 4A-I). The efficiency of Cre-mediated *Mek1* deletion in explants was assessed by IHC. No MEK1 staining was detected in lung mesenchyme from mutants (Fig. 4J,K). Moreover, the proportion of proliferative cells in lung mesenchyme and epithelium remained unchanged in *Mek1*$^{flox/flox}$;*Mek2*$^{-/-}$;*Dermo1*$^{+/Cre}$ explants, indicating that the phenotype observed *in vivo* was not recapitulated *in vitro* (Fig. 4L-N).

Treatment of lung explants with FGF9 causes increased mesenchymal growth and luminal dilation of epithelial tubules (del Moral et al., 2006; Yin et al., 2011). We investigated the response of *Mek1*$^{flox/flox}$;*Mek2*$^{-/-}$;*Dermo1*$^{+/Cre}$ explants to FGF9. Both control and mutant lung explants cultured with FGF9 showed bud dilation and reduced epithelial branching, suggesting that the FGF9 effect on lung mesenchyme is mediated by MEK-independent intracellular signaling pathways (supplementary material Fig. S6).

Rat lung explant experiments have shown that pharmacological MEK inhibition reduces *in vitro* lung branching (Kling et al., 2002). We repeated this study with lung explants from E12.5 wild-type mice treated with the MEK inhibitor PD98059. In agreement with the previous analyses, PD98059 treatment diminished lung explant branching (Fig. 4O-U). Thus, lung hypoplasia in *Mek1*$^{flox/flox}$;*Mek2*$^{-/-}$;*Dermo1*$^{+/Cre}$ embryos might be a consequence of the omphalocele and/or the abnormal skeleton, both participating in the reduced intrathoracic space. Our data also point towards a role of the ERK/MAPK pathway in the lung epithelium for a normal branching process.

Mek1 epithelial inactivation on a *Mek2* null background results in lung agenesis

To directly address the epithelial role of MEK1 and MEK2 in lung branching, *Mek1* was conditionally inactivated in *Mek2*$^{-/-}$ lung epithelium using *Shh*^{Cre} mice (supplementary material Fig. S1E-H; Harfe et al., 2004; Harris et al., 2006). All *Mek1*$^{flox/flox}$;*Mek2*$^{-/-}$;*Shh*$^{+/Cre}$ newborns became cyanotic and died at birth (Fig. 5A). E18.5, *Mek1*^{floxflox};*Mek2*$^{-/-}$;*Shh*$^{+/Cre}$ embryos presented a shortened trachea with a reduced number of cartilage rings (Fig. 5F,G). The trachea split into truncated primary bronchi without further branching, failing to form lungs (Fig. 5B-E). No lung phenotype was observed in *Mek1*$^{+flox}$;*Mek2*$^{-/-}$;*Shh*$^{+/Cre}$ and *Mek1*$^{flox/flox}$;*Mek2*$^{+/-}$;*Shh*$^{+/Cre}$ embryos or mice. Thus, the presence of one functional *Mek* allele either in lung mesenchyme or in lung epithelium is sufficient for correct lung development, maturation and function.

The efficiency of Cre-mediated *Mek1* deletion was confirmed by the epithelial loss of MEK1 and pERK expression in *Mek1*$^{flox/flox}$;*Mek2*$^{-/-}$;*Shh*$^{+/Cre}$ specimens (supplementary material Fig. S4G-J). To identify the causes of lung agenesis, cell proliferation was assessed at E12.5 using cell cycle progression markers. Reduced cyclin D1 immunostaining was observed in lung epithelium from *Mek1*$^{flox/flox}$;*Mek2*$^{-/-}$;*Shh*$^{+/Cre}$ mutants in contrast to the strong expression seen in controls (Fig. 5H,I). Ki67 labeling in lung epithelium and mesenchyme was also diminished in mutants (Fig. 5J,K). Finally, a significantly decreased number of BrdU-positive cells was detected in the lung epithelium and mesenchyme of *Mek1*$^{flox/flox}$;*Mek2*$^{-/-}$;*Shh*$^{+/Cre}$ mutants (Fig. 5L-N). The reduced epithelial cell proliferation correlated with an increased number of epithelial cells positive for the cell cycle inhibitor p27^{Kip1} (Fig. 5O,P). Thus, the ERK/MAPK pathway in lung epithelium is essential for cyclin D1 expression and cell cycle progression.

Cell apoptosis was examined. Compared with controls, E12.5 *Mek1*$^{flox/flox}$;*Mek2*$^{-/-}$;*Shh*$^{+/Cre}$ mutants presented substantial cleaved caspase 3 immunostaining along the epithelium of the truncated bronchi, with the strongest signal at the distal tip. Apoptosis was also observed in the distal mesenchyme of lung rudiments (Fig. 5Q,R). The ERK/MAPK pathway inhibits caspase 9 activity by direct phosphorylation at Thr 125, blocking caspase 3 activation and subsequent apoptosis (Allan et al., 2003). In *Mek1*$^{flox/flox}$;*Mek2*$^{-/-}$;*Shh*$^{+/Cre}$ mutants, phosphorylation of caspase 9 was reduced in bronchial buds when compared with controls (Fig. 5S,T). These data provide compelling evidence that the ERK/MAPK pathway is essential for lung branching by directly controlling cell proliferation and survival.

Lung agenesis in *Mek1*$^{flox/flox}$;*Mek2*$^{-/-}$;*Shh*$^{+/Cre}$ mutants resembled *Fgf10* and *Fgfr2b* mutant lung phenotypes (De Moerlooze et al., 2000; Min et al., 1998; Sekine et al., 1999). *In vitro* experiments have shown that *Bmp4* expression is induced at the tip of growing buds in response to mesenchymal FGF10 participating in branching regulation (Weaver et al., 2000). The *Bmp4*-reduced expression in lungs from E12.5 *Mek1*$^{flox/flox}$;*Mek2*$^{-/-}$;*Shh*$^{+/Cre}$ mutants demonstrated that a functional ERK/MAPK pathway in lung epithelium is required to transduce FGF10-induced *Bmp4* expression *in vivo* (supplementary material Fig. S7).

Trachea formation requires both mesenchymal and epithelial ERK/MAPK signaling

Cartilage rings constitute the supporting wall of the upper airways during breathing, thereby maintaining the patency of the lumen. E18.5 *Mek1*$^{flox/flox}$;*Mek2*$^{-/-}$;*Dermo1*$^{+/Cre}$ embryos displayed a thinner trachea without cartilage rings along the trachea and primary bronchi. Only a few isolated nests of cartilage cells were seen (Fig. 6A,B). Cre activity from the *Dermo1*^{Cre} allele was detected in the cartilage nodules, demonstrating that the tracheal phenotype of *Mek1*$^{flox/flox}$;*Mek2*$^{-/-}$;*Dermo1*$^{+/Cre}$ embryos was cell-autonomous (Fig. 6C). In controls, activated ERK was found in cartilage nodules, thus further supporting the requirement of the ERK/MAPK pathway in tracheal cartilage formation (Fig. 6D).

We analyzed the expression of SRY (sex-determining region Y)-box 9 (SOX9), a master regulator of chondrogenesis essential for

Development (2014) 141, 3197-3211 doi:10.1242/dev.110254

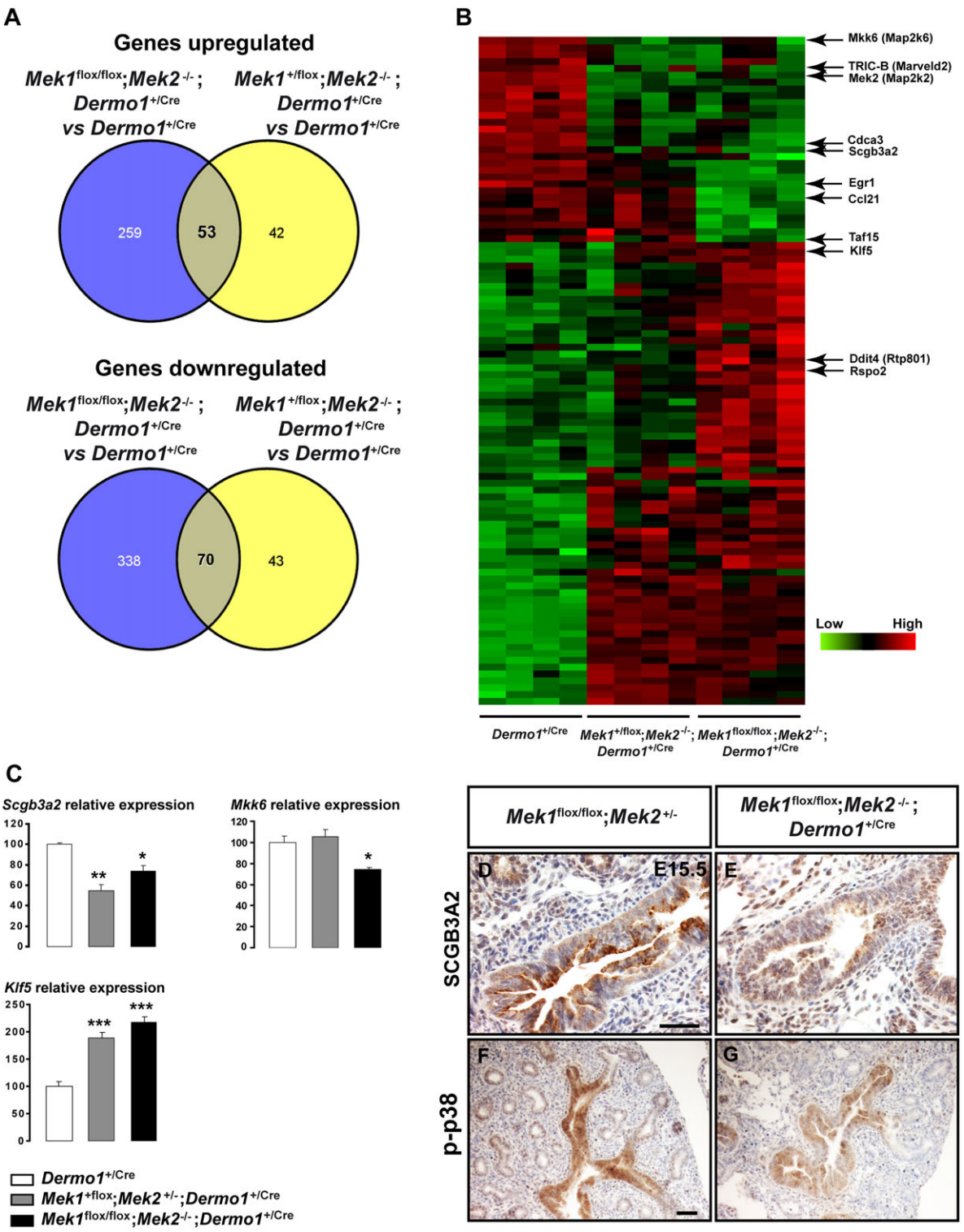

Fig. 3. Differential gene expression in lungs from E15.5 *Mek1*$^{+/flox}$;*Mek2*$^{-/-}$;*Dermo1*$^{+/Cre}$ and *Mek1*$^{flox/flox}$;*Mek2*$^{-/-}$;*Dermo1*$^{+/Cre}$ embryos. (A) Venn diagrams representing the overlap of genes differentially expressed (Benjamini–Hochberg-adjusted $P<0.05$) between genotypes. (B) Heat map analysis displaying deregulated genes (>1.5-fold; $P<0.05$). Genes mentioned in the text are indicated by arrows. (C) qRT-PCR analyses for *Scgb3a2*, *Mkk6* and *Klf5* confirmed the microarray data. Values are expressed as mean±s.e.m. (D-G) SCGB3A2 (D,E) and phospho-p38 (F,G) IHC showed a substantial reduction of both markers in lung epithelium from E15.5 *Mek1*$^{flox/flox}$;*Mek2*$^{-/-}$;*Dermo1*$^{+/Cre}$ specimens compared with controls. Scale bars: 50 µm.

patterning and formation of the tracheal cartilage (Park et al., 2010). In E14.5 controls, the segmented SOX9 expression showed the pattern of the future cartilage rings. *Mek1*$^{flox/flox}$;*Mek2*$^{-/-}$;*Dermo1*$^{+/Cre}$ embryos displayed a continuous SOX9 expression, indicating the lack of formation of the precartilage nodules (Fig. 6E,F). Accumulation of cartilage-specific type II collagen, which normally takes place following mesenchymal condensation, did not occur in mutant airways (Fig. 6G,H). qRT-PCR analyses revealed reduced

Development (2014) 141, 3197-3211 doi:10.1242/dev.110254

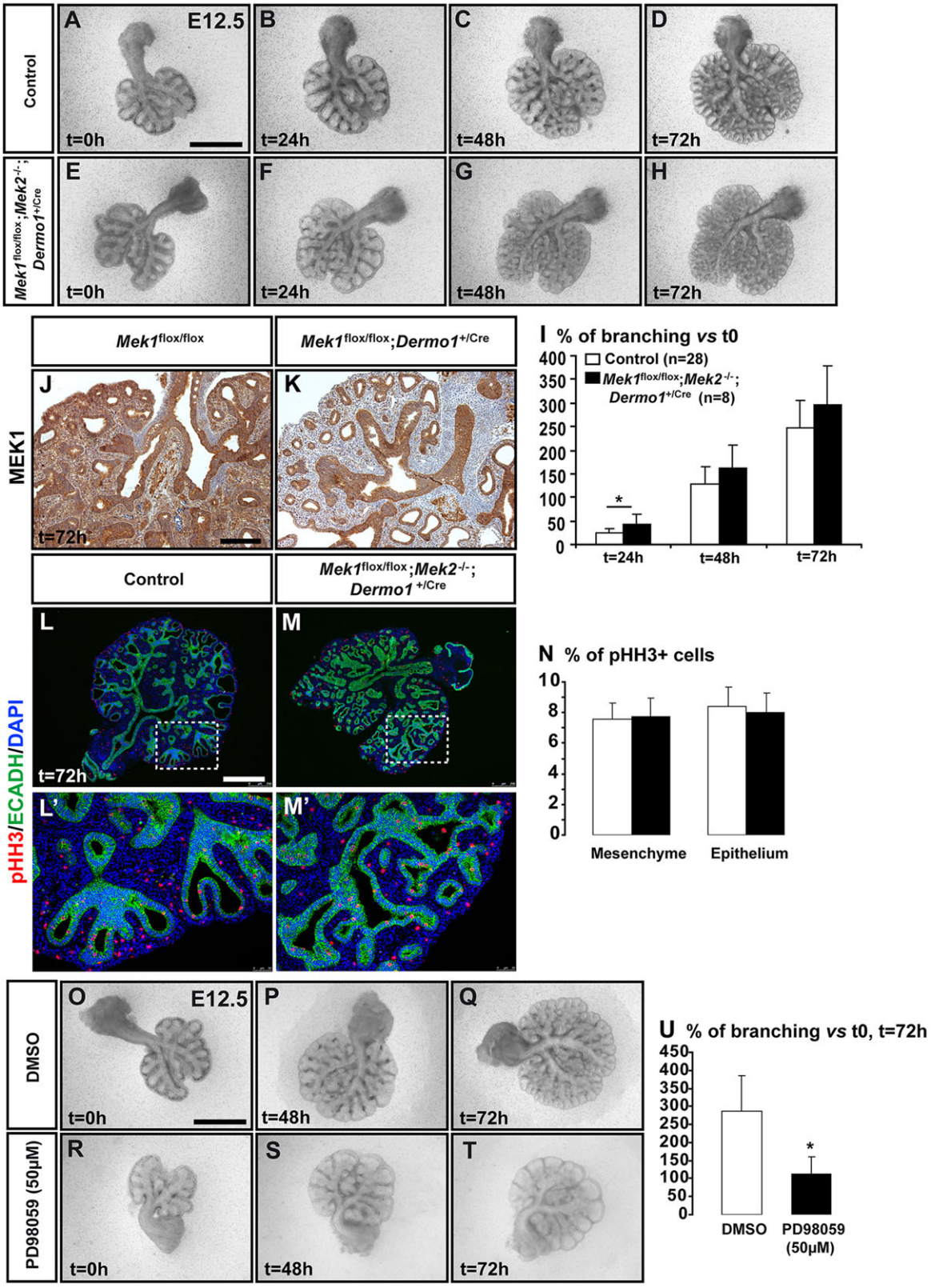

Fig. 4. *In vitro* rescue of the lung branching defect of *Mek1*$^{flox/flox}$;*Mek2*$^{-/-}$;*Dermo1*$^{Cre/+}$ embryos. (A-H) Lung explants from E12.5 controls (A-D) and *Mek1*$^{flox/flox}$;*Mek2*$^{-/-}$;*Dermo1*$^{+/Cre}$ (E-H) embryos maintained in culture for 3 days. (I) Quantification of the number of terminal buds at 24, 48 and 72 h is expressed as branching increase (%) versus t0. The loss of *Mek* function in lung mesenchyme did not impair lung branching. At least eight lungs were analyzed per condition. (J,K) MEK1 IHC confirmed *Mek1* deletion in lung mesenchyme of *Mek1*$^{flox/flox}$;*Mek2*$^{-/-}$;*Dermo1*$^{+/Cre}$ lung explants at 72 h. (L-N) Co-immunofluorescence with anti-E-cadherin (green) and anti-pHH3 (red) antibodies showed similar proliferation rate in *Mek1*$^{flox/flox}$;*Mek2*$^{-/-}$;*Dermo1*$^{+/Cre}$ explants versus controls at 72 h. (O-U) Treatment of wild-type lung explants with the MEK inhibitor PD98059 significantly reduced lung branching (*n*=3-5/group). Scale bars: 1 mm (A-H,O-T), 500 μm (L,M), 200 μm (J,K). Values are expressed as mean±s.d.

Development (2014) 141, 3197-3211 doi:10.1242/dev.110254

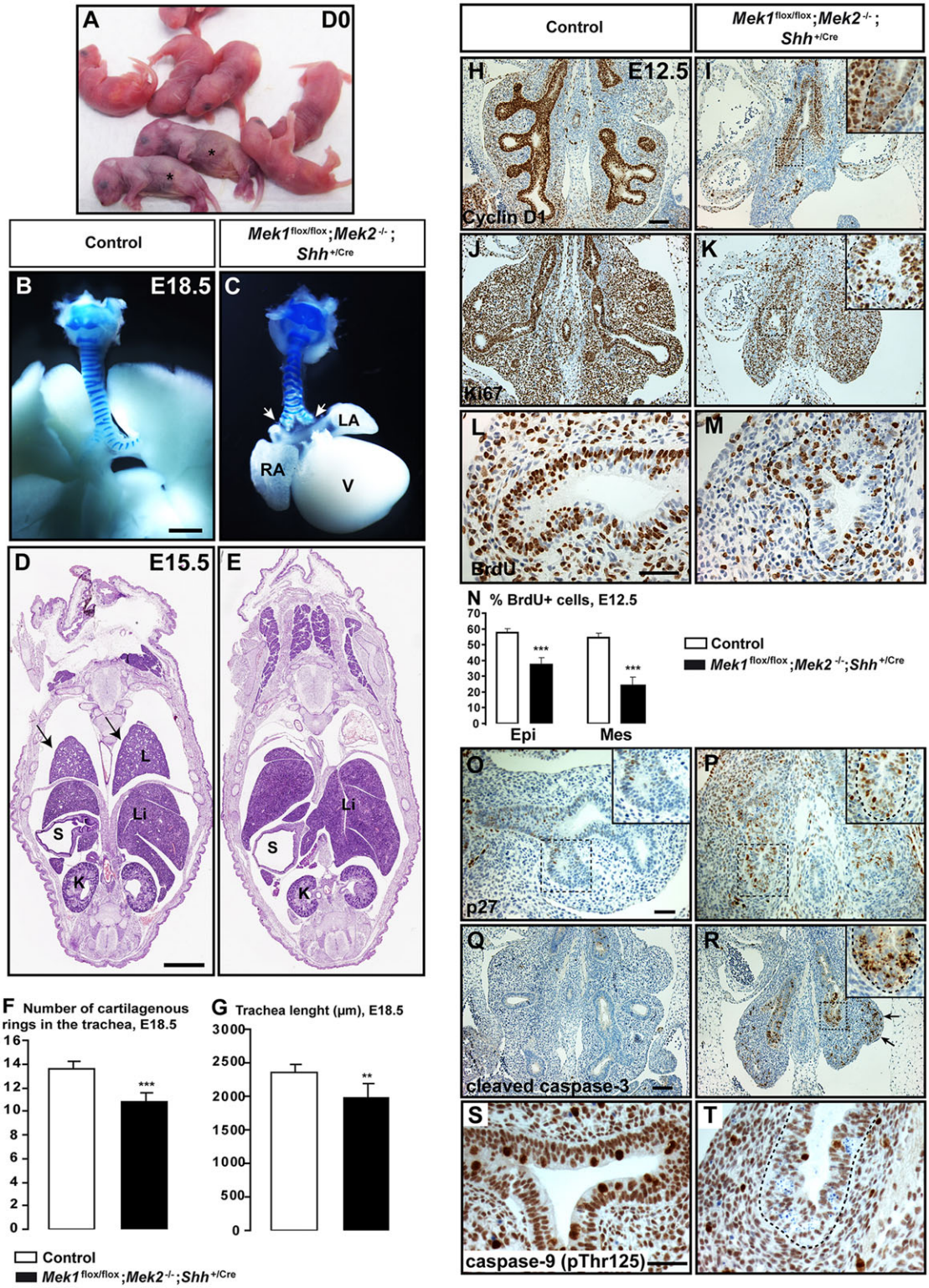

Fig. 5. Lung agenesis in *Mek1*$^{flox/flox}$;*Mek2*$^{-/-}$;*Shh*$^{+/Cre}$ embryos. (A) *Mek1*$^{flox/flox}$;*Mek2*$^{-/-}$;*Shh*$^{+/Cre}$ newborn mice (asterisks) became cyanotic and died at birth. (B,C) Alcian Blue staining of the respiratory tract from E18.5 *Mek1*$^{flox/flox}$;*Mek2*$^{-/-}$;*Shh*$^{+/Cre}$ embryos revealed lung agenesis. Arrows indicate the caudal end of primary bronchi without further branching. (D,E) H&E-stained frontal sections of E15.5 control and *Mek1*$^{flox/flox}$;*Mek2*$^{-/-}$;*Shh*$^{+/Cre}$ embryos showed the lack of lungs (arrows in D) in mutant specimens. (F,G) Reduced number of cartilage rings and shorter trachea were observed in E18.5 *Mek1*$^{flox/flox}$;*Mek2*$^{-/-}$;*Shh*$^{+/Cre}$ specimens (n=6-17/group). (H-N) Cyclin D1 (H,I), Ki67 (J,K) and BrdU (L-N) IHC assays revealed decreased cell proliferation in lung epithelium and mesenchyme of E12.5 *Mek1*$^{flox/flox}$;*Mek2*$^{-/-}$;*Shh*$^{+/Cre}$ lungs (n=5/group). (O,P) p27^{kip1} IHC showed increased expression of the cell-cycle inhibitor in lung epithelium of E12.5 *Mek1*$^{flox/flox}$;*Mek2*$^{-/-}$;*Shh*$^{+/Cre}$ mutants. (Q,R) Cleaved caspase 3 IHC revealed apoptosis in lung epithelium and mesenchyme of E12.5 *Mek1*$^{flox/flox}$;*Mek2*$^{-/-}$;*Shh*$^{+/Cre}$ mutants. Arrows indicate cleaved caspase 3-positive cells in mesenchyme. (S,T) IHC for phospho-caspase 9 at Thr 125 showed reduced staining in *Mek1*$^{flox/flox}$;*Mek2*$^{-/-}$;*Shh*$^{+/Cre}$ bronchial buds. Scale bars: 1 mm (B-E), 100 µm (H-K,Q,R), 50 µm (L,M,O,P,S,T). Values are expressed as mean±s.d. K, kidney; L, lung; LA, left atrium; Li, liver; RA, right atrium; S, stomach; V, ventricle.

Development (2014) 141, 3197-3211 doi:10.1242/dev.110254

expression levels of the chondrogenic regulator trio, *Sox5*, *Sox6* and *Sox9*, and their downstream targets, aggrecan (*Acan*) and collagen type II alpha 1 (*Col2a1*), in upper airways from E18.5 *Mek1*$^{flox/flox}$;*Mek2*$^{-/-}$;*Dermo1*$^{+/Cre}$ embryos (Fig. 6I,J). Thus, the lack of ERK/MAPK function in the upper airway mesenchyme of *Mek1*$^{flox/flox}$;*Mek2*$^{-/-}$;*Dermo1*$^{+/Cre}$ mutants perturbed the expression of major regulators of chondrogenesis, resulting in failure of mesenchymal condensation and subsequent tracheal cartilage formation, thus causing the flaccidity of the trachea.

The trachea of *Mek1*$^{flox/flox}$;*Mek2*$^{-/-}$;*Shh*$^{+/Cre}$ mutants was shorter with fewer cartilage rings (Fig. 5F,G). We assessed whether *Mek* epithelial deletion had direct effects on the tracheal epithelium integrity. In E12.5-E18.5 controls, the trachea was lined by a pseudostratified columnar epithelium. At E18.5, the epithelium is normally composed of ciliated cells, club cells and few goblet cells, covering a layer of p63 (*Tcp1* – Mouse Genome Informatics)-positive basal cells (Fig. 7; supplementary material Fig. S8). In *Mek1*$^{flox/flox}$;*Mek2*$^{-/-}$;*Shh*$^{+/Cre}$ mutants, cells failed to maintain their stratification around E14.5 (supplementary material Fig. S8D,H). E18.5 mutants exhibited a simple squamous epithelium virtually devoid of basal, goblet and ciliated cells, with only a few club cells (Fig. 7). The lack of basal cells was also observed at E14.5, indicating a crucial role for the ERK/MAPK pathway in basal cell differentiation (supplementary material Fig. S8). This correlated with the diminution in basal cells in mutants overexpressing an FGFR2b dominant negative form (Volckaert et al., 2013).

No staining was detected in *Mek1*$^{flox/flox}$;*Mek2*$^{-/-}$;*Shh*$^{+/Cre}$ mutants with the stage-specific embryonic antigen 1 (SSEA1; *Fut4* – Mouse Genome Informatics), a marker of pluripotent stem cells (Fig. 7G,H; Henderson et al., 2002). To explain the lack of tracheal epithelial cell differentiation, we hypothesized that the loss of *Mek* function could lead to a downregulation of SOX2 expression, preventing differentiation of embryonic airway progenitors into specific lineages (Que et al., 2009). At E18.5, *Mek1*$^{flox/flox}$;*Mek2*$^{-/-}$;*Shh*$^{+/Cre}$ mutants presented rare SOX2-positive cells along the trachea. At earlier stages, all tracheal epithelial cells expressed SOX2 but at a lower intensity, suggesting that the ERK/MAPK pathway is required to maintain SOX2 expression at levels sufficient to allow cell differentiation (Fig. 7I,J; supplementary material Fig. S8). Together, our findings demonstrate that the ERK/MAPK pathway is essential for the maintenance of a tracheal progenitor cell population and for the correct tracheal epithelial cell differentiation. They also emphasize the absolute requirement of mesenchymal and epithelial expression of *Mek1* and *Mek2* in trachea formation.

Epithelial inactivation of *Erk1* and *Erk2* reproduces the *Mek1*;*Mek2* lung epithelial phenotype

We wanted to determine whether the respiratory tract phenotype arising from the epithelial inactivation of both *Mek* genes would be recapitulated upon inactivation of the downstream effectors *Erk1* (*Mapk3* – Mouse Genome Informatics) and *Erk2* (*Mapk1* – Mouse Genome Informatics). E18.5 *Erk1*$^{-/-}$;*Erk2*$^{flox/flox}$;*Shh*$^{+/Cre}$ embryos exhibited the same phenotypes as *Mek1*$^{flox/flox}$;*Mek2*$^{-/-}$;*Shh*$^{+/Cre}$ embryos: lung agenesis, abnormal tracheal epithelial differentiation and death at birth (Fig. 8). These data underscored that the MEK-ERK module acts as a linear pathway, in which ERK1 and ERK2 are the sole effectors of MEK kinases in the lung epithelium.

DISCUSSION

MEK isoforms possess unique functions as reflected by the distinct phenotypes of the *Mek1* and *Mek2* single mutants (Bélanger et al., 2003; Giroux et al., 1999). This specificity can be explained by the exclusive roles and/or the different spatial distribution or levels of MEK proteins. Our genetic studies on *Mek* gene function in respiratory tract formation demonstrated that the presence of only one functional *Mek* allele in the mesenchyme or in the epithelium is sufficient to support normal development and to allow survival of mutant pups. Thus, *Mek1* and *Mek2* genes display redundant functions during lung morphogenesis. A similar observation could be made for the role of *Erk1* and *Erk2* in lung epithelium.

The phenotypes resulting from the mesenchymal ablation of *Mek* genes were anticipated due to the large spectrum of actions of the ligands trafficking via the ERK/MAPK pathway. For instance, abnormal body wall formation and omphalocele were reported in mice carrying conditional mutations in both *Fgfr1* and *Fgfr2* genes (Nichol et al., 2011). Normal lung growth requires adequate space in the thoracic cavity and appropriate tonic and cyclic distending forces originating in part from fetal breathing movements (Kotecha, 2000). Mesenchymal *Mek* mutation caused kyphosis and omphalocele, mimicking human pathological conditions that can impose a significant physical restriction on lung growth and function (Argyle, 1989; McMaster et al., 2007). In addition to *Fgfr1*;*Fgfr2* compound mutants, abnormal body wall formation was seen in mice carrying conditional mutations in the *Alk3* gene encoding a BMP type I receptor, and the *Alk5* gene encoding a Tgfβ type I receptor (Matsunobu et al., 2009; Sun et al., 2007). BMP4 and TGFβ were shown to activate the ERK/MAPK pathway in various experimental conditions (Hough et al., 2012; Lee et al., 2007). Therefore, it is possible that the ERK/MAPK pathway acts as a convergence point for the FGF-, BMP- and TGFβ-driven signaling cascades in the mesenchyme to control ventral body wall closure.

Lung explant cultures demonstrated that defective branching and cell proliferation of *Mek1*$^{flox/flox}$;*Mek2*$^{-/-}$;*Dermo1*$^{+/Cre}$ specimens can be rescued *in vitro*. This indicates that the lung has the capacity to correctly develop in absence of a functional ERK/MAPK pathway in lung mesenchyme at the pseudoglandular stage. These results identify the mechanical restriction due to dysmorphic rib cage and severe omphalocele as a probable cause of the pulmonary hypoplasia that challenged the neonatal survival of *Mek1*$^{flox/flox}$;*Mek2*$^{-/-}$;*Dermo1*$^{+/Cre}$ pups. However, a role of *Mek* genes in lung mesenchyme at later stages of lung development cannot be excluded.

In *Mek1*$^{flox/flox}$;*Mek2*$^{-/-}$;*Shh*$^{+/Cre}$ embryos, the specification of the primary lung field occurred with the formation of the trachea and its bifurcation to produce primary bronchial buds. However, the lack of *Mek* function in lung epithelium did not allow further development resulting in lung agenesis. Thus, even though the early steps of the specification of the trachea and lung progenitors in the ventral foregut were reported to necessitate WNT and FGF signals, the latter was not transduced via the ERK/MAPK pathway as suggested by our data (Goss et al., 2009; Serls et al., 2005). Although recently challenged, the dynamic pattern of *Fgf10* expression to sites of prospective bud formation and the FGF10 ability to induce epithelial proliferation and budding in lung organ cultures have led to the hypothesis that FGF10 controls the directional outgrowth of lung buds during branching morphogenesis. In agreement with this, lung agenesis was reported in *Fgf10* and *Fgfr2b* mutant embryos, which both failed to develop primary bronchial buds (Bellusci et al., 1997; De Moerlooze et al., 2000; Harris et al., 2006; Min et al., 1998; Sekine et al., 1999; Volckaert et al., 2013). Our results support the notion that the tracheal bifurcation mediated by the FGF10-FGFR2b interaction is also ERK/MAPK-independent, as the epithelial mutation with the *Shh*^{Cre} allele occurs before lung formation onset (Harris-Johnson et al., 2009). Thus, trachea formation and its

Development (2014) 141, 3197-3211 doi:10.1242/dev.110254

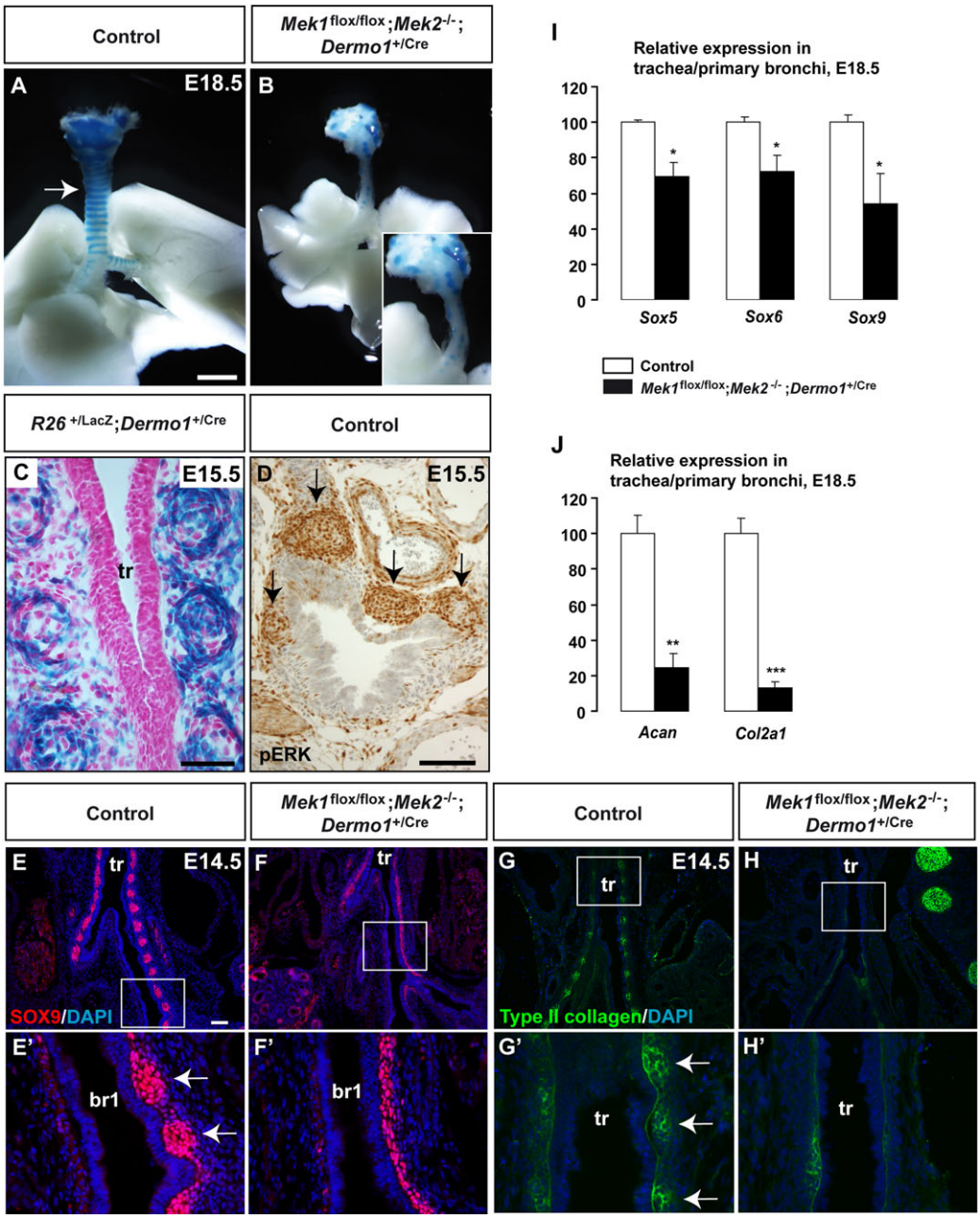

Fig. 6. Patterning defects of the trachea cartilage rings from *Mek1*$^{flox/flox}$;*Mek2*$^{-/-}$;*Dermo1*$^{+/Cre}$ embryos. (A,B) The *Mek* mutations in lung mesenchyme resulted in the lack of cartilage rings along the trachea and primary bronchi as shown by Alcian Blue staining of E18.5 control and *Mek1*$^{flox/flox}$;*Mek2*$^{-/-}$;*Dermo1*$^{+/Cre}$ respiratory tracts. (C) E15.5 *R26*$^{+/LacZ}$;*Dermo1*$^{+/Cre}$ embryos displayed β-galactosidase activity in tracheal mesenchyme and cartilage nodules. (D) Phospho-ERK-positive cells were detected in cartilage nodules (arrows) from E15.5 wild-type embryos. (E,F) Unsegmented SOX9 expression was observed along the upper airways of E14.5 *Mek1*$^{flox/flox}$;*Mek2*$^{-/-}$;*Dermo1*$^{+/Cre}$ embryos compared with controls. (G,H) Accumulation of cartilage-specific type II collagen did not occur in mutant airways. (I,J) qRT-PCR analyses for the *Sox5*, *Sox6* and *Sox9* transcription factor genes (I) and for their targets *Acan* and *Col2a1* (J) in upper airways from E18.5 *Mek1*$^{flox/flox}$;*Mek2*$^{-/-}$;*Dermo1*$^{+/Cre}$ mutants. Values are expressed as mean±s.e.m. br1, primary bronchi; tr, trachea. Scale bars: 1 mm (A,B), 200 µm (E-H), 100 µm (D), 50 µm (C).

branching into primary bronchi do not depend on the epithelial ERK/MAPK pathway, whereas the subsequent branching events seem to do. This concurs with the idea that trachea bifurcation and the following ramifications arise in distinct anatomical fields that require different genetic networks (Metzger et al., 2008).

Decreased cell proliferation combined with augmented apoptosis underlie lung agenesis in *Mek1*$^{flox/flox}$;*Mek2*$^{-/-}$;*Shh*$^{+/Cre}$ embryos, two cell processes that are under the direct control of the ERK/MAPK pathway. It has been shown that the ERK/MAPK cascade regulates progression through the cell cycle by stimulating increased cyclin D1 levels that signal continued proliferation (Lavoie et al., 1996). This necessitates the phosphorylation by ERK of the MYC transcription factor, which, once activated, promotes the transcription of the cyclin D1 gene *Ccnd1* (Mouse Genome Informatics) (Daksis et al., 1994). In parallel, the ERK/MAPK pathway can suppress the levels of the cdk inhibitor p27^{Kip1} via the proteasome pathway, which impacts on the rate of cell cycle progression (Schepers et al., 2005; Stacey, 2010). Consequently,

Development (2014) 141, 3197-3211 doi:10.1242/dev.110254

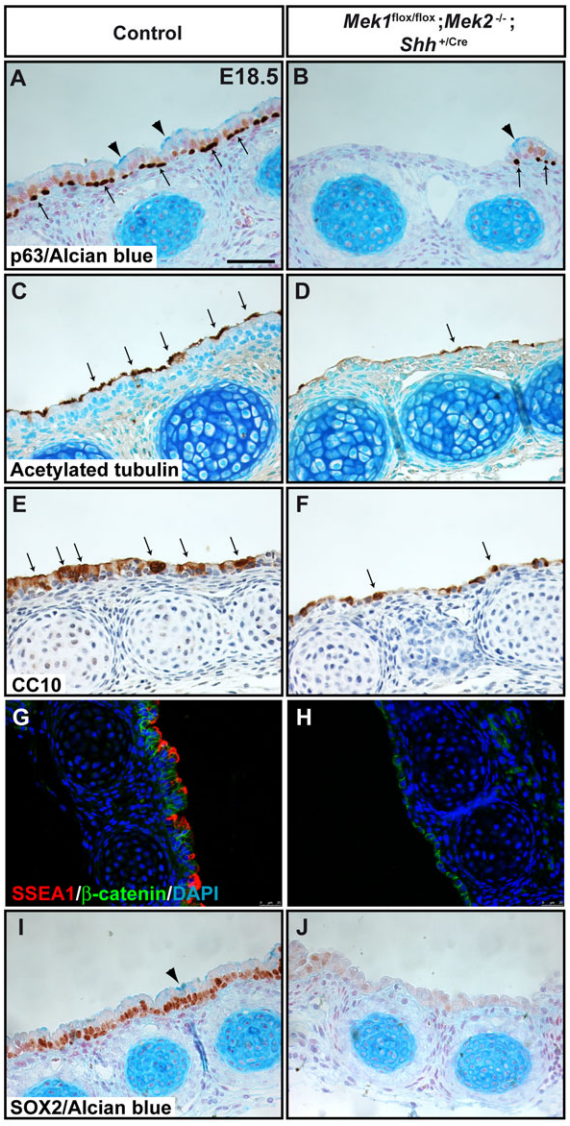

Fig. 7. *Mek* genes control upper airway epithelial cell differentiation. (A,B) p63, (C,D) acetylated tubulin and (E,F) CC10 IHC assays revealed basal, ciliated and club cells, respectively (arrows). Mucus-producing goblet cells were detected with Alcian Blue (A,B; arrowheads). The *Mek* mutation in the tracheal epithelium caused a loss of basal, club and ciliated cells. The pseudostratified epithelium normally seen in controls was absent in *Mek1*$^{flox/flox}$;*Mek2*$^{-/-}$;*Shh*$^{+/Cre}$ specimens. (G,H) Co-immunofluorescence with anti-β-catenin (green) and anti-SSEA1 (red) antibodies showed the lack of progenitor cells within the tracheal epithelium of mutant embryos. (I,J) SOX2 IHC revealed a loss of SOX2 expression in the tracheal epithelium from mutants. Scale bar: 50 µm.

in absence of functional MEK proteins in lung epithelium, *Ccnd1* expression was reduced and p27^{Kip1} levels were increased in mutant lungs, leading to cell cycle arrest and decreased proliferation.

The ERK/MAPK pathway is also involved in the control of apoptosis by directly controlling the activity of the initiator protease caspase 9 via its phosphorylation at Thr 125 by ERK. Phosphorylated caspase 9 is inefficient to process caspase 3 proteolytic activation and the ensuing apoptosis (Allan et al., 2003). In *Mek1*$^{flox/flox}$;*Mek2*$^{-/-}$;*Shh*$^{+/Cre}$ embryos, the levels of phosphorylated caspase 9 were diminished and, consequently, those of cleaved caspase 3 were augmented, thereby triggering increased apoptosis. Together, our findings provide a mechanistic insight into how the absence of *Mek* function in the lung epithelium directly affects cell proliferation and survival. It thus causes a profound deregulation of the proliferation/apoptosis balance, a likely explanation for the observed lung agenesis (Fig. 9).

The loss of *Mek* function either in the mesenchyme or the epithelium impacted on trachea formation, thus affecting the targeted cell layer and revealing the importance of the cell-autonomous role of the ERK/MAPK pathway during trachea development. Tracheas from *Mek1*$^{flox/flox}$;*Mek2*$^{-/-}$;*Dermo1*$^{+/Cre}$ embryos manifest a near-complete absence of C-shaped cartilage rings along the entire length of the upper airways, thereby providing a putative mouse model for primary tracheomalacia, a weakness of the tracheal walls causing life-threatening conditions (Carden et al., 2005). Tracheal cartilage development results from a multistep process, involving mesenchymal cell proliferation, aggregation and condensation into pre-cartilaginous nodules, which subsequently differentiate into chondrocytes to form cartilage. Several genes, including *Hoxa5*, *Shh*, *Fgf10*, *Fgfr2*, *Gli2* and *Gli3*, *Fstl1* and *Tmem16a* (*Ano1* – Mouse Genome Informatics), were identified as key players in tracheal cartilage development based on mutant mice characterization (Aubin et al., 1997; Geng et al., 2011; Motoyama et al., 1998; Rock et al., 2008; Sala et al., 2011). As most of these genes encode growth factors or transcriptional regulators, the mesenchymal deletion of *Mek* genes represents one of the first examples demonstrating the crucial role of intracellular signaling molecules in tracheal chondrogenesis. Our results strongly suggest that this action is mediated by SOX9. FGF as well as a MEK constitutive active form enhance *Sox9* expression and SOX9 transcriptional activity on a SOX9-dependent enhancer in primary chondrocytes (Murakami et al., 2000). The twofold decrease in *Sox9* transcript levels in the upper airways of *Mek1*$^{flox/flox}$;*Mek2*$^{-/-}$;*Dermo1*$^{+/Cre}$ embryos specimens supports a direct effect of ERK/MAPK signaling on *Sox9* expression. This reduction in gene dosage might be sufficient to perturb cartilage formation, as *Sox9*$^{+/-}$ embryos die perinatally with severe cartilage hypoplasia (Bi et al., 2001). Similarly, *SOX9* haploinsufficiency in humans causes campomelic dysplasia characterized by severe skeletal dysmorphologies (Wunderle et al., 1998). Alternatively, the absence of *Mek* function in tracheal mesenchyme might affect SOX9 phosphorylation, known to increase its DNA binding and transcriptional activity (Huang et al., 2000). In support of this notion, activated ERK1 and ERK2 can physically interact with SOX9 in chondrocyte nuclei, raising the possibility that the ERK/MAPK cascade directly promotes SOX9 phosphorylation, thus modulating its transcriptional role (Shakibaei et al., 2006). Therefore, it is not surprising that the loss of *Mek* function in lung mesenchyme with its negative impact on *Sox9* expression resulted in the downregulation of SOX9 targets, such as SOX5 and SOX6, two transcriptional regulators that act as a trio together with SOX9 to control chondrogenesis (Akiyama et al., 2002). Consequently, the diminished expression of the three regulators led to the downregulation of cartilage-specific genes, like the proteoglycan aggrecan (*Acan*) and the extracellular matrix protein collagen *Col2a1*, resulting in absence of mesenchymal condensation and subsequent tracheal cartilage formation, which causes the flaccidity of the trachea (Fig. 9).

Conversely, tracheas from *Mek1*$^{flox/flox}$;*Mek2*$^{-/-}$;*Shh*$^{+/Cre}$ and *Erk1*$^{-/-}$;*Erk2*$^{flox/flox}$;*Shh*$^{+/Cre}$ embryos exhibit a correct patterning of the cartilage rings, but a profound impairment of tracheal epithelial differentiation. This contrasts with the phenotypes of *Fgf10*$^{-/-}$ and *Fgfr2b*$^{-/-}$ mutants, which both exhibited a shortened

Development (2014) 141, 3197-3211 doi:10.1242/dev.110254

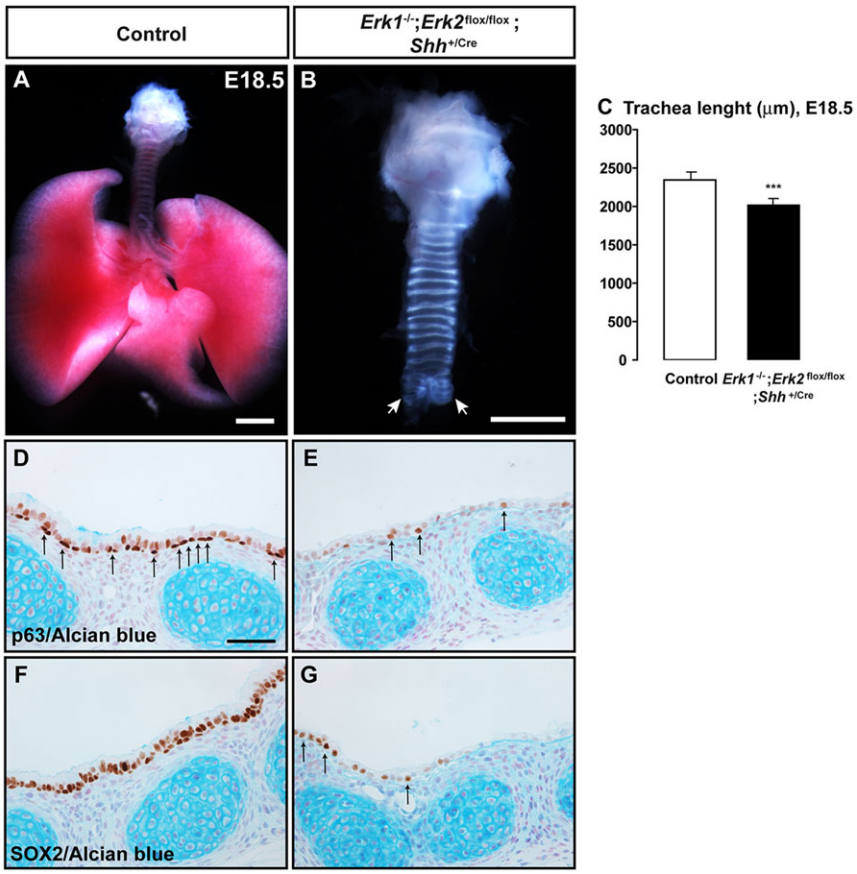

Fig. 8. Lung agenesis and defective epithelial cell differentiation phenotypes are recapitulated after *Erk*-specific deletion in lung epithelium. (A,B) Macroscopic view of lungs from E18.5 control and *Erk1*$^{-/-}$;*Erk2*$^{flox/flox}$;*Shh*$^{+/Cre}$ embryos. Mutant mice exhibited lung agenesis and arrows indicated the truncated primary bronchi. The patterning of the cartilage rings was normal. (C) The length of the trachea from E18.5 *Erk1*$^{-/-}$;*Erk2*$^{flox/flox}$;*Shh*$^{+/Cre}$ embryos was significantly reduced compared with controls. Values are expressed as mean±s.d. IHC for p63 (D,E) and SOX2 (F,G) showed the reduced number of basal cells and the dramatic decrease of SOX2 expression, respectively, in the tracheal epithelium of E18.5 *Erk1*$^{-/-}$;*Erk2*$^{flox/flox}$;*Shh*$^{+/Cre}$ embryos. Scale bars: 1 mm (A,B), 50 µm (D-G).

trachea with defective cartilage patterning. It has been shown that the mesenchymal *Fgf10* expression activates FGFR2b signaling in the tracheal epithelium to drive cartilage formation via expression of *Shh*. However, the trachea from *Fgf10*$^{-/-}$ embryos did not present major alterations in epithelial differentiation (Sala et al., 2011). The divergence in phenotypic traits raises questions about the identity of the ligand-receptor pair(s) trafficking via the ERK/MAPK pathway in the tracheal epithelium (Fig. 9).

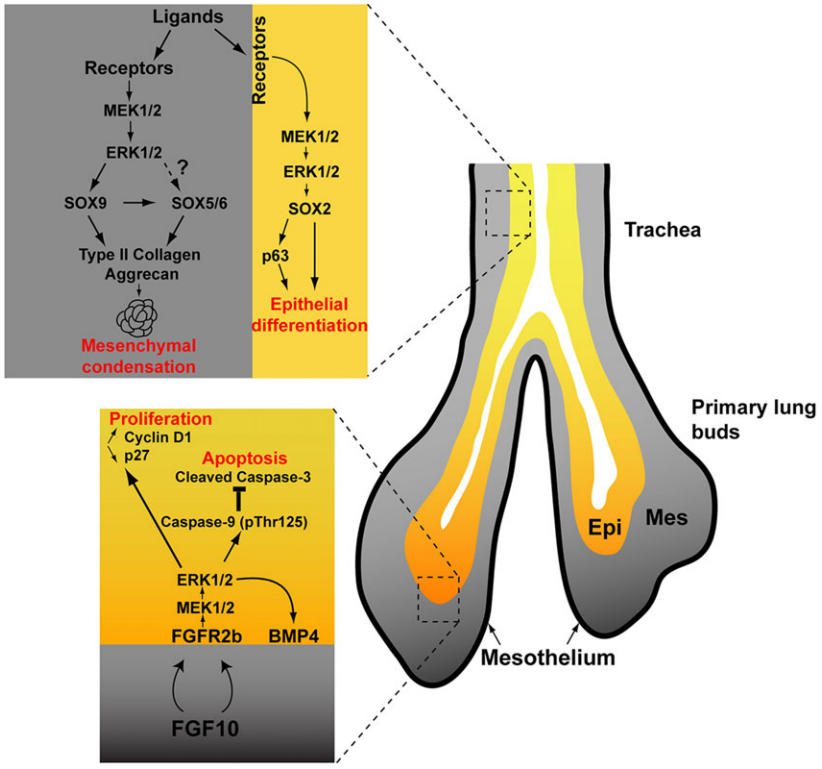

Fig. 9. A model for the action of the ERK/MAPK pathway during the development of the respiratory tract. In the trachea and primary bronchi, the mesenchymal activation of the ERK/MAPK cascade is required for the regulation of expression of the SOX5, SOX6 and SOX9 trio and the subsequent mesenchymal condensation and cartilage formation. Expression of *Mek1* and *Mek2* in the tracheal epithelium governs epithelial cell differentiation via the control of SOX2 expression. Ligand(s) and receptor(s) are unknown. In the lung, mesenchymal FGF10 binds to FGFR2b expressed in the branching epithelium and signals via the ERK/MAPK cascade to promote cell proliferation and to prevent cell apoptosis. Epi, epithelium; Mes, mesenchyme.

Development (2014) 141, 3197-3211 doi:10.1242/dev.110254

The formation of an undifferentiated squamous epithelium lacking the expression of specific markers for basal, club, ciliated and mucus cells in *Mek1*$^{flox/flox}$;*Mek2*$^{-/-}$;*Shh*$^{+/Cre}$ and *Erk1*$^{-/-}$;*Erk2*$^{flox/flox}$;*Shh*$^{+/Cre}$ embryos can be attributed to the absence of expression of SOX2, a key transcriptional regulator of tracheal epithelium differentiation (Que et al., 2009). The loss of SOX2 expression in tracheal epithelial cells in *Mek1*$^{flox/flox}$;*Mek2*$^{-/-}$;*Shh*$^{+/Cre}$ and *Erk1*$^{-/-}$;*Erk2*$^{flox/flox}$;*Shh*$^{+/Cre}$ mutants is intriguing, as it indicates new, unsuspected roles for the ERK/MAPK pathway in progenitor cell maintenance and SOX2-mediated airway epithelial differentiation. Further works are needed to fully elucidate the underlying signaling mechanisms (Fig. 9).

In conclusion, we present new evidence that the ERK/MAPK pathway plays specific roles in the epithelium and the mesenchyme of the developing respiratory tract. Whereas its direct function in lung mesenchyme remains to be clearly established, the absence of the ERK/MAPK pathway in lung epithelium is crucial for lung formation, and it phenocopies lung agenesis also observed in *Fgf10* and *Fgfr2b* mutant mice. Decreased epithelial cell proliferation coupled with increased cell death appears to be the mechanism responsible for lung agenesis. In the trachea, the ERK/MAPK pathway plays a cell-autonomous role in each cell layer, transducing signals in the mesenchyme for correct tracheal chondrogenesis and in the epithelium for progenitor cell maintenance and differentiation. These phenotypes diverge from those observed in *Fgf10* and *Fgfr2* mutants, indicating that other ligand-receptor pair(s) trafficking via the ERK/MAPK pathway are involved in trachea formation.

MATERIALS AND METHODS

Mice, genotyping and tissue collection

The *Mek1*$^{flox/flox}$ and *Mek2*$^{-/-}$ mouse lines were described previously (Bélanger et al., 2003; Bissonauth et al., 2006). The *Erk1*$^{-/-}$ and *Erk2*$^{flox/flox}$ mouse lines were obtained from Dr Meloche (IRIC, Université de Montréal, Montréal, Canada; Pagés et al., 1999; Voisin et al., 2010). The *Rosa26* reporter line (*Gt(ROSA)26Sor*^{tm1Sor}) and the *Shh*^{Cre} deleter strain (*Shh*$^{tm1(EGFP/cre)Cjt}$) were purchased (Jackson Laboratory; Harfe et al., 2004; Soriano, 1999). *Dermo1*^{Cre} mice were provided by Dr Ornitz (Washington University, St. Louis, USA; Yu et al., 2003). For the mesenchymal ablation of *Mek1* on a *Mek2*-null background, *Mek1*$^{flox/flox}$;*Mek2*$^{-/-}$;*Dermo1*$^{+/Cre}$ specimens were generated by breeding *Mek1*$^{flox/+}$;*Mek2*$^{+/-}$;*Dermo1*$^{+/Cre}$ with *Mek1*$^{flox/flox}$;*Mek2*$^{-/-}$ mice. Similar breeding steps were carried out to produce *Mek1*$^{flox/flox}$;*Mek2*$^{-/-}$;*Shh*$^{+/Cre}$ and *Erk1*$^{-/-}$;*Erk2*$^{flox/flox}$;*Shh*$^{+/Cre}$ specimens for the *Mek1* and *Erk2* epithelial deletions, respectively. As only individuals carrying the *Mek1*$^{flox/flox}$;*Mek2*$^{-/-}$;*Dermo1*$^{+/Cre}$, *Mek1*$^{flox/flox}$;*Mek2*$^{-/-}$;*Shh*$^{+/Cre}$ and *Erk1*$^{-/-}$;*Erk2*$^{flox/flox}$;*Shh*$^{+/Cre}$ genotypes presented defects, all other genotypes are referred to hereafter as controls. The age of the embryos was estimated by considering the morning of the day of the vaginal plug as E0.5. Experimental specimens were genotyped by Southern blot and PCR analyses. Lungs from control and mutant embryos were collected at E12.5, E14.5, E15.5, E18.5 and D0. For adult specimens, lungs were dissected, instilled with 4% cold paraformaldehyde and paraffin-embedded. For RNA extraction, lungs were snap-frozen in N_2. Experiments were performed according to the guidelines of the Canadian Council on Animal Care and approved by the institutional animal care committee.

Mouse embryo lung explant cultures

Lungs were collected from E12.5 mouse embryos and cultured for 72 h on porous membranes (8 µm pore size) in 24-well plates (del Moral and Warburton, 2010). The number of terminal buds at 0, 24, 48 and 72 h at the periphery of explants was counted and the branching increase (%) at each time point was calculated as:

$$(\text{Branches}_{24,\ 48\ \text{or}\ 72\ \text{h}} - \text{Branches}_{0\ \text{h}})/\text{Branches}_{0\ \text{h}} \times 100.$$

Exogenous recombinant mouse FGF9 (rmFGF9) was added to explants at a concentration of 200 ng/ml (del Moral et al., 2006). Stock solutions of PD98059 (20 mM) were prepared in DMSO and added to medium at a final concentration of 50 µM. Medium was changed daily.

Histology, IHC and immunofluorescence (IF) analyses

Paraffin-embedded embryos or lungs were sectioned at 4 µm for E12.5-E18.5 specimens and at 6 µm for older specimens. Morphology was analyzed by hematoxylin and eosin (H&E) staining. Immunostaining experiments were performed (Boucherat et al., 2012). Slides were counterstained with either Alcian Blue (for detection of acid mucus-producing cells) and nuclear Fast Red, methyl green or hematoxylin. For IF studies, nuclei were visualized by DAPI staining. Primary and secondary antibodies used are listed in supplementary material Table S1.

Proliferation and apoptosis analyses

Proliferation and apoptotic indices were obtained by counting the number of pHH3-, BrdU- and cleaved caspase 3-immunoreactive cells, respectively, divided by the total cell number in lung epithelium or mesenchyme for each section analyzed. Five to six random fields were taken for an average number of 300 cells per field, from four to five embryos per genotype. For BrdU analyses, pregnant females were injected intraperitoneally with 100 µg/g body weight, and embryos were collected 1 h later.

β-galactosidase staining

Whole-mount detection of β-galactosidase activity in E8.5-E12.5 embryos and in dissected lung from E12.5 embryos was performed (Trainor et al., 1999). Cryostat sections (10 µm) of E12.5 embryos were processed for X-gal staining (Boucherat et al., 2012).

In situ hybridization

RNA *in situ* hybridization was performed on paraffin sections of E12.5 embryos (Simmons et al., 2008). A 486-bp *SmaI-BstE*II fragment containing 5′ non-coding and coding sequences from the mouse *Bmp4* gene was used for synthesizing the digoxigenin-labeled riboprobe. The experiment was performed on four specimens per genotype.

Quantitative RT-PCR (qRT-PCR) experiments

Total RNA was isolated from the trachea/primary bronchi and the lungs of individual E15.5 and E18.5 embryos, and qRT-PCR experiments were performed (Boucherat et al., 2012). Four to six specimens were used for each genotype tested. Primer sequences are listed in supplementary material Table S2.

Microarray analysis

Total RNA was isolated from lungs of E15.5 *Dermo1*$^{+/Cre}$, *Mek1*$^{+/flox}$;*Mek2*$^{-/-}$;*Dermo1*$^{+/Cre}$ and *Mek1*$^{flox/flox}$;*Mek2*$^{-/-}$;*Dermo1*$^{+/Cre}$ embryos (n=4/genotype). RNA quality and quantity assessment, cDNA probe preparation, hybridization to the Illumina MouseWG-6 v2.0 Expression BeadChip and image scan were performed at the Genome Quebec Innovation Centre at McGill University (Montréal, Canada). Data were normalized using log2 transformation followed by quantile normalization with the R/lumi package in BioConductor (Du et al., 2008). Raw and normalized data were uploaded in the NCBI Gene Expression Omnibus database (http://www.ncbi.nlm.nih.gov/projects/geo) with the accession number GSE51643 according to MIAME standards (Edgar et al., 2002). Significantly modulated probes were identified using the empirical Bayes statistics available in limma (Smyth, 2004). Probes were considered to be significantly modulated when the Benjamini–Hochberg-adjusted P<0.05.

Morphometry analyses

Total lung surface and the number and area of epithelial tubules were measured using Adobe Photoshop CS3 software. Total lung mesenchymal surface was obtained by subtracting the airway tubule area from the total lung area. The number of acini was normalized according to the total lung area.

Development (2014) 141, 3197-3211 doi:10.1242/dev.110254

Statistical analyses

Student's *t*-test was performed for comparative studies. A significance level inferior to 5% ($P<0.05$) was considered statistically significant. *$P<0.05$, **$P<0.01$, ***$P<0.001$.

Acknowledgements

We thank Dr F. Costantini for insightful comments on the manuscript, Drs S. Meloche and D. Ornitz for mouse lines, Drs S. Kimura and G. Singh for antibodies, Dr L. Robertson for *in situ* riboprobe and E. Paquet for the analysis of microarray data.

Competing interests

The authors declare no competing financial interests.

Author contributions

O.B., J.C. and L.J. designed the experiments; O.B., V.N. and F.-A.B.-S. performed the experiments; O.B., V.N., F.-A.B.-S., J.C. and L.J. analyzed the data; O.B., J.C. and L.J. wrote the paper.

Funding

This work was supported by grants from the Canadian Institutes of Health Research [MOP-15139 to L.J., MOP-97801 to J.C.].

Supplementary material

Supplementary material available online at http://dev.biologists.org/lookup/suppl/doi:10.1242/dev.110254/-/DC1

References

Akiyama, H., Chaboissier, M.-C., Martin, J. F., Schedl, A. and de Crombrugghe, B. (2002). The transcription factor Sox9 has essential roles in successive steps of the chondrocyte differentiation pathway and is required for expression of Sox5 and Sox6. *Genes Dev.* **16**, 2813-2828.

Allan, L. A., Morrice, N., Brady, S., Magee, G., Pathak, S. and Clarke, P. R. (2003). Inhibition of caspase-9 through phosphorylation at Thr 125 by ERK MAPK. *Nat. Cell Biol.* **5**, 647-654.

Argyle, J. C. (1989). Pulmonary hypoplasia in infants with giant abdominal wall defects. *Fetal Pediatr. Pathol.* **9**, 43-55.

Aubin, J., Lemieux, M., Tremblay, M., Bérard, J. and Jeannotte, L. (1997). Early postnatal lethality in Hoxa-5 mutant mice is attributable to respiratory tract defects. *Dev. Biol.* **192**, 432-445.

Ayad, N. G., Rankin, S., Murakami, M., Jebanathirajah, J., Gygi, S. and Kirschner, M. W. (2003). Tome-1, a trigger of mitotic entry, is degraded during G1 via the APC. *Cell* **113**, 101-113.

Bélanger, L.-F., Roy, S., Tremblay, M., Brott, B., Steff, A.-M., Mourad, W., Hugo, P., Erikson, R. and Charron, J. (2003). Mek2 is dispensable for mouse growth and development. *Mol. Cell. Biol.* **23**, 4778-4787.

Bell, S. M., Schreiner, C. M., Wert, S. E., Mucenski, M. L., Scott, W. J. and Whitsett, J. A. (2008). R-spondin 2 is required for normal laryngeal-tracheal, lung and limb morphogenesis. *Development* **135**, 1049-1058.

Bellusci, S., Grindley, J., Emoto, H., Itoh, N. and Hogan, B. L. (1997). Fibroblast growth factor 10 (FGF10) and branching morphogenesis in the embryonic mouse lung. *Development* **124**, 4867-4878.

Bi, W., Huang, W., Whitworth, D. J., Deng, J. M., Zhang, Z., Behringer, R. R. and de Crombrugghe, B. (2001). Haploinsufficiency of Sox9 results in defective cartilage primordia and premature skeletal mineralization. *Proc. Natl. Acad. Sci. USA* **98**, 6698-6703.

Bissonauth, V., Roy, S., Gravel, M., Guillemette, S. and Charron, J. (2006). Requirement for Map2k1 (Mek1) in extra-embryonic ectoderm during placentogenesis. *Development* **133**, 3429-3440.

Boucherat, O., Chakir, J. and Jeannotte, L. (2012). The loss of Hoxa5 function promotes Notch-dependent goblet cell metaplasia in lung airways. *Biol. Open* **1**, 677-691.

Boucherat, O., Montaron, S., Berube-Simard, F.-A., Aubin, J., Philippidou, P., Wellik, D. M., Dasen, J. S. and Jeannotte, L. (2013). Partial functional redundancy between Hoxa5 and Hoxb5 paralog genes during lung morphogenesis. *Am. J. Physiol. Lung Cell. Mol. Physiol.* **304**, L817-L830.

Carden, K. A., Boiselle, P. M., Waltz, D. A. and Ernst, A. (2005). Tracheomalacia and tracheobronchomalacia in children and adults: an in-depth review. *Chest* **127**, 984-1005.

Christison-Lagay, E. R., Kelleher, C. M. and Langer, J. C. (2011). Neonatal abdominal wall defects. *Semin. Fetal Neonatal Med.* **16**, 164-172.

Daksis, J. I., Lu, R. Y., Facchini, L. M., Marhin, W. W. and Penn, L. J. (1994). Myc induces cyclin D1 expression in the absence of de novo protein synthesis and links mitogen-stimulated signal transduction to the cell cycle. *Oncogene* **9**, 3635-3645.

De Moerlooze, L., Spencer-Dene, B., Revest, J. M., Hajihosseini, M., Rosewell, I. and Dickson, C. (2000). An important role for the IIIb isoform of fibroblast growth factor receptor 2 (FGFR2) in mesenchymal-epithelial signalling during mouse organogenesis. *Development* **127**, 483-492.

del Moral, P. M. and Warburton, D. (2010). Explant culture of mouse embryonic whole lung, isolated epithelium, or mesenchyme under chemically defined conditions as a system to evaluate the molecular mechanism of branching morphogenesis and cellular differentiation. *Methods Mol. Biol.* **633**, 71-79.

del Moral, P.-M., De Langhe, S. P., Sala, F. G., Veltmaat, J. M., Tefft, D., Wang, K., Warburton, D. and Bellusci, S. (2006). Differential role of FGF9 on epithelium and mesenchyme in mouse embryonic lung. *Dev. Biol.* **293**, 77-89.

Du, P., Kibbe, W. A. and Lin, S. M. (2008). lumi: a pipeline for processing Illumina microarray. *Bioinformatics* **24**, 1547-1548.

Edgar, R., Domrachev, M. and Lash, A. E. (2002). Gene Expression Omnibus: NCBI gene expression and hybridization array data repository. *Nucleic Acids Res.* **30**, 207-210.

Geng, Y., Dong, Y., Yu, M., Zhang, L., Yan, X., Sun, J., Qiao, L., Geng, H., Nakajima, M., Furuichi, T. et al. (2011). Follistatin-like 1 (Fstl1) is a bone morphogenetic protein (BMP) 4 signaling antagonist in controlling mouse lung development. *Proc. Natl. Acad. Sci. USA* **108**, 7058-7063.

Giroux, S., Tremblay, M., Bernard, D., Cadrin-Girard, J.-F., Aubry, S., Larouche, L., Rousseau, S., Huot, J., Landry, J., Jeannotte, L. et al. (1999). Embryonic death of Mek1-deficient mice reveals a role for this kinase in angiogenesis in the labyrinthine region of the placenta. *Curr. Biol.* **9**, 369-376.

Goss, A. M., Tian, Y., Tsukiyama, T., Cohen, E. D., Zhou, D., Lu, M. M., Yamaguchi, T. P. and Morrisey, E. E. (2009). Wnt2/2b and beta-catenin signaling are necessary and sufficient to specify lung progenitors in the foregut. *Dev. Cell* **17**, 290-298.

Harfe, B. D., Scherz, P. J., Nissim, S., Tian, H., McMahon, A. P. and Tabin, C. J. (2004). Evidence for an expansion-based temporal Shh gradient in specifying vertebrate digit identities. *Cell* **118**, 517-528.

Harris, K. S., Zhang, Z., McManus, M. T., Harfe, B. D. and Sun, X. (2006). Dicer function is essential for lung epithelium morphogenesis. *Proc. Natl. Acad. Sci. USA* **103**, 2208-2213.

Harris-Johnson, K. S., Domyan, E. T., Vezina, C. M. and Sun, X. (2009). beta-Catenin promotes respiratory progenitor identity in mouse foregut. *Proc. Natl. Acad. Sci. USA* **106**, 16287-16292.

Henderson, J. K., Draper, J. S., Baillie, H. S., Fishel, S., Thomson, J. A., Moore, H. and Andrews, P. W. (2002). Preimplantation human embryos and embryonic stem cells show comparable expression of stage-specific embryonic antigens. *Stem Cells* **20**, 329-337.

Hough, C., Radu, M. and Doré, J. J. E. (2012). Tgf-beta induced Erk phosphorylation of smad linker region regulates smad signaling. *PLoS ONE* **7**, e42513.

Huang, W., Zhou, X., Lefebvre, V. and de Crombrugghe, B. (2000). Phosphorylation of SOX9 by cyclic AMP-dependent protein kinase A enhances SOX9's ability to transactivate a Col2a1 chondrocyte-specific enhancer. *Mol. Cell. Biol.* **20**, 4149-4158.

Huang, D. W., Sherman, B. T. and Lempicki, R. A. (2009). Systematic and integrative analysis of large gene lists using DAVID bioinformatics resources. *Nat. Protoc.* **4**, 44-57.

Kling, D. E., Lorenzo, H. K., Trbovich, A. M., Kinane, T. B., Donahoe, P. K. and Schnitzer, J. J. (2002). MEK-1/2 inhibition reduces branching morphogenesis and causes mesenchymal cell apoptosis in fetal rat lungs. *Am. J. Physiol. Lung Cell. Mol. Physiol.* **282**, L370-L378.

Kotecha, S. (2000). Lung growth for beginners. *Paediatr. Respir. Rev.* **1**, 308-313.

Kurotani, R., Tomita, T., Yang, Q., Carlson, B. A., Chen, C. and Kimura, S. (2008). Role of secretoglobin 3A2 in lung development. *Am. J. Respir. Crit. Care Med.* **178**, 389-398.

Lavoie, J. N., L'Allemain, G., Brunet, A., Muller, R. and Pouyssegur, J. (1996). Cyclin D1 expression is regulated positively by the p42/p44MAPK and negatively by the p38/HOGMAPK pathway. *J. Biol. Chem.* **271**, 20608-20616.

Lee, M. K., Pardoux, C., Hall, M. C., Lee, P. S., Warburton, D., Qing, J., Smith, S. M. and Derynck, R. (2007). TGF-beta activates Erk MAP kinase signalling through direct phosphorylation of ShcA. *EMBO J.* **26**, 3957-3967.

Li, X., Newbern, J. M., Wu, Y., Morgan-Smith, M., Zhong, J., Charron, J. and Snider, W. D. (2012). MEK is a key regulator of gliogenesis in the developing brain. *Neuron* **75**, 1035-1050.

Lindahl, P., Karlsson, L., Hellstrom, M., Gebre-Medhin, S., Willetts, K., Heath, J. K. and Betsholtz, C. (1997). Alveogenesis failure in PDGF-A-deficient mice is coupled to lack of distal spreading of alveolar smooth muscle cell progenitors during lung development. *Development* **124**, 3943-3953.

Liu, Y., Martinez, L., Ebine, K. and Abe, M. K. (2008). Role for mitogen-activated protein kinase p38 alpha in lung epithelial branching morphogenesis. *Dev. Biol.* **314**, 224-235.

Matsunobu, T., Torigoe, K., Ishikawa, M., de Vega, S., Kulkarni, A. B., Iwamoto, Y. and Yamada, Y. (2009). Critical roles of the TGF-beta type I receptor ALK5 in perichondrial formation and function, cartilage integrity, and osteoblast differentiation during growth plate development. *Dev. Biol.* **332**, 325-338.

McMaster, M. J., Glasby, M. A., Singh, H. and Cunningham, S. (2007). Lung function in congenital kyphosis and kyphoscoliosis. *J. Spinal Disord. Tech.* **20**, 203-208.

Metzger, R. J., Klein, O. D., Martin, G. R. and Krasnow, M. A. (2008). The branching programme of mouse lung development. *Nature* **453**, 745-750.
Min, H., Danilenko, D. M., Scully, S. A., Bolon, B., Ring, B. D., Tarpley, J. E., DeRose, M. and Simonet, W. S. (1998). Fgf-10 is required for both limb and lung development and exhibits striking functional similarity to Drosophila branchless. *Genes Dev.* **12**, 3156-3161.
Morrisey, E. E. and Hogan, B. L. M. (2010). Preparing for the first breath: genetic and cellular mechanisms in lung development. *Dev. Cell* **18**, 8-23.
Motoyama, J., Liu, J., Mo, R., Ding, Q., Post, M. and Hui, C.-C. (1998). Essential function of Gli2 and Gli3 in the formation of lung, trachea and oesophagus. *Nat. Genet.* **20**, 54-57.
Murakami, S., Kan, M., McKeehan, W. L. and de Crombrugghe, B. (2000). Up-regulation of the chondrogenic Sox9 gene by fibroblast growth factors is mediated by the mitogen-activated protein kinase pathway. *Proc. Natl. Acad. Sci. USA* **97**, 1113-1118.
Nadeau, V., Guillemette, S., Belanger, L.-F., Jacob, O., Roy, S. and Charron, J. (2009). Map2k1 and Map2k2 genes contribute to the normal development of syncytiotrophoblasts during placentation. *Development* **136**, 1363-1374.
Newbern, J., Zhong, J., Wickramasinghe, R. S., Li, X., Wu, Y., Samuels, I., Cherosky, N., Karlo, J. C., O'Loughlin, B., Wikenheiser, J. et al. (2008). Mouse and human phenotypes indicate a critical conserved role for ERK2 signaling in neural crest development. *Proc. Natl. Acad. Sci. USA* **105**, 17115-17120.
Nichol, P. F., Corliss, R. F., Tyrrell, J. D., Graham, B., Reeder, A. and Saijoh, Y. (2011). Conditional mutation of fibroblast growth factor receptors 1 and 2 results in an omphalocele in mice associated with disruptions in ventral body wall muscle formation. *J. Pediatr. Surg.* **46**, 90-96.
Pagés, G., Guérin, S., Grall, D., Bonino, F., Smith, A., Anjuere, F., Auberger, P. and Pouysségur, J. (1999). Defective thymocyte maturation in p44 MAP kinase (Erk 1) knockout mice. *Science* **286**, 1374-1377.
Park, J., Zhang, J. J. R., Moro, A., Kushida, M., Wegner, M. and Kim, P. C. W. (2010). Regulation of Sox9 by Sonic Hedgehog (Shh) is essential for patterning and formation of tracheal cartilage. *Dev. Dyn.* **239**, 514-526.
Que, J., Luo, X., Schwartz, R. J. and Hogan, B. L. M. (2009). Multiple roles for Sox2 in the developing and adult mouse trachea. *Development* **136**, 1899-1907.
Raman, M., Chen, W. and Cobb, M. H. (2007). Differential regulation and properties of MAPKs. *Oncogene* **26**, 3100-3112.
Rock, J. R., Futtner, C. R. and Harfe, B. D. (2008). The transmembrane protein TMEM16A is required for normal development of the murine trachea. *Dev. Biol.* **321**, 141-149.
Rock, J. R., Barkauskas, C. E., Cronce, M. J., Xue, Y., Harris, J. R., Liang, J., Noble, P. W. and Hogan, B. L. M. (2011). Multiple stromal populations contribute to pulmonary fibrosis without evidence for epithelial to mesenchymal transition. *Proc. Natl. Acad. Sci. USA* **108**, E1475-E1483.
Sala, F. G., Del Moral, P.-M., Tiozzo, C., Al Alam, D., Warburton, D., Grikscheit, T., Veltmaat, J. M. and Bellusci, S. (2011). FGF10 controls the patterning of the tracheal cartilage rings via Shh. *Development* **138**, 273-282.
Schepers, H., Wierenga, A. T. J., Eggen, B. J. L. and Vellenga, E. (2005). Oncogenic Ras blocks transforming growth factor-beta-induced cell-cycle arrest by degradation of p27 through a MEK/Erk/SKP2-dependent pathway. *Exp. Hematol.* **33**, 747-757.
Scholl, F. A., Dumesic, P. A., Barragan, D. I., Harada, K., Bissonauth, V., Charron, J. and Khavari, P. A. (2007). Mek1/2 MAPK kinases are essential for Mammalian development, homeostasis, and raf-induced hyperplasia. *Dev. Cell* **12**, 615-629.
Sekine, K., Ohuchi, H., Fujiwara, M., Yamasaki, M., Yoshizawa, T., Sato, T., Yagishita, N., Matsui, D., Koga, Y., Itoh, N. et al. (1999). Fgf10 is essential for limb and lung formation. *Nat. Genet.* **21**, 138-141.
Serls, A. E., Doherty, S., Parvatiyar, P., Wells, J. M. and Deutsch, G. H. (2005). Different thresholds of fibroblast growth factors pattern the ventral foregut into liver and lung. *Development* **132**, 35-47.
Shakibaei, M., Seifarth, C., John, T., Rahmanzadeh, M. and Mobasheri, A. (2006). Igf-I extends the chondrogenic potential of human articular chondrocytes in vitro: molecular association between Sox9 and Erk1/2. *Biochem. Pharmacol.* **72**, 1382-1395.
Simmons, D. G., Natale, D. R. C., Begay, V., Hughes, M., Leutz, A. and Cross, J. C. (2008). Early patterning of the chorion leads to the trilaminar trophoblast cell structure in the placental labyrinth. *Development* **135**, 2083-2091.
Smyth, G. K. (2004). Linear models and empirical bayes methods for assessing differential expression in microarray experiments. *Stat. Appl. Genet. Mol. Biol.* **3**, Article3.
Soriano, P. (1999). Generalized lacZ expression with the ROSA26 Cre reporter strain. *Nat. Genet.* **21**, 70-71.
Stacey, D. W. (2010). Three observations that have changed our understanding of Cyclin D1 and $p27^{Kip1}$ in cell cycle control. *Genes Cancer* **1**, 1189-1199.
Sun, J., Liu, Y.-H., Chen, H., Nguyen, M. P., Mishina, Y., Upperman, J. S., Ford, H. R. and Shi, W. (2007). Deficient Alk3-mediated BMP signaling causes prenatal omphalocele-like defect. *Biochem. Biophys. Res. Commun.* **360**, 238-243.
Tada, Y., Majka, S., Carr, M., Harral, J., Crona, D., Kuriyama, T. and West, J. (2007). Molecular effects of loss of BMPR2 signaling in smooth muscle in a transgenic mouse model of PAH. *Am. J. Physiol. Lung Cell. Mol. Physiol.* **292**, L1556-L1563.
Tang, N., Marshall, W. F., McMahon, M., Metzger, R. J. and Martin, G. R. (2011). Control of mitotic spindle angle by the RAS-regulated ERK1/2 pathway determines lung tube shape. *Science* **333**, 342-345.
Trainor, P. A., Zhou, S. X., Parameswaran, M., Quinlan, G. A., Gordon, M., Sturm, K. and Tam, P. P. (1999). Application of lacZ transgenic mice to cell lineage studies. *Methods Mol. Biol.* **97**, 183-200.
Voisin, L., Saba-El-Leil, M. K., Julien, C., Fremin, C. and Meloche, S. (2010). Genetic demonstration of a redundant role of extracellular signal-regulated kinase 1 (ERK1) and ERK2 mitogen-activated protein kinases in promoting fibroblast proliferation. *Mol. Cell. Biol.* **30**, 2918-2932.
Volckaert, T., Campbell, A., Dill, E., Li, C., Minoo, P. and De Langhe, S. (2013). Localized Fgf10 expression is not required for lung branching morphogenesis but prevents differentiation of epithelial progenitors. *Development* **140**, 3731-3742.
Wan, H., Luo, F., Wert, S. E., Zhang, L., Xu, Y., Ikegami, M., Maeda, Y., Bell, S. M. and Whitsett, J. A. (2008). Kruppel-like factor 5 is required for perinatal lung morphogenesis and function. *Development* **135**, 2563-2572.
Weaver, M., Dunn, N. R. and Hogan, B. L. (2000). Bmp4 and Fgf10 play opposing roles during lung bud morphogenesis. *Development* **127**, 2695-2704.
Wunderle, V. M., Critcher, R., Hastie, N., Goodfellow, P. N. and Schedl, A. (1998). Deletion of long-range regulatory elements upstream of SOX9 causes campomelic dysplasia. *Proc. Natl. Acad. Sci. USA* **95**, 10649-10654.
Yamashita, S., Tai, P., Charron, J., Ko, C. and Ascoli, M. (2011). The Leydig cell MEK/ERK pathway is critical for maintaining a functional population of adult Leydig cells and for fertility. *Mol. Endocrinol.* **25**, 1211-1222.
Yamazaki, D., Komazaki, S., Nakanishi, H., Mishima, A., Nishi, M., Yazawa, M., Yamazaki, T., Taguchi, R. and Takeshima, H. (2009). Essential role of the TRIC-B channel in Ca2+ handling of alveolar epithelial cells and in perinatal lung maturation. *Development* **136**, 2355-2361.
Yang, Y., Goldstein, B. G., Nakagawa, H. and Katz, J. P. (2007). Kruppel-like factor 5 activates MEK/ERK signaling via EGFR in primary squamous epithelial cells. *FASEB J.* **21**, 543-550.
Yin, Y., Wang, F. and Ornitz, D. M. (2011). Mesothelial- and epithelial-derived FGF9 have distinct functions in the regulation of lung development. *Development* **138**, 3169-3177.
Yoshida, T., Mett, I., Bhunia, A. K., Bowman, J., Perez, M., Zhang, L., Gandjeva, A., Zhen, L. J., Chukwueke, U., Mao, T. et al. (2010). Rtp801, a suppressor of mTOR signaling, is an essential mediator of cigarette smoke-induced pulmonary injury and emphysema. *Nat. Med.* **16**, 767-773.
Yu, K., Xu, J., Liu, Z., Sosic, D., Shao, J., Olson, E. N., Towler, D. A. and Ornitz, D. M. (2003). Conditional inactivation of FGF receptor 2 reveals an essential role for FGF signaling in the regulation of osteoblast function and bone growth. *Development* **130**, 3063-3074.